



Afdelingen for Bærende Konstruktioner  
Department of Structural Engineering  
Danmarks Tekniske Højskole · Technical University of Denmark

DESIGN PROPOSAL FOR  
HIGH STRENGTH CONCRETE SECTIONS  
SUBJECTED TO FLEXURAL AND AXIAL LOADS

NICHOLAUS HOLKMANN OLSEN

Serie R

No 233

1990

**DESIGN PROPOSAL FOR  
HIGH STRENGTH CONCRETE SECTIONS  
SUBJECTED TO FLEXURAL AND AXIAL LOADS**

**NICHOLAUS HOLKMANN OLSEN**

**Design Proposal for High Strength Concrete Sections subjected to Flex-  
ural and Axial Loads**

Copyright © by Nicholaus Holkmann Olsen 1990

Tryk:

Afdelingen for Bærende Konstruktioner

Danmarks Tekniske Højskole

Lyngby

ISBN 87-7740-053-4

## PREFACE

This report has been prepared as one part of the thesis required to obtain the degree of "teknisk licentiat", equivalent to the Ph.D. degree.

This thesis consist of this report and the following three reports:

- Heat-Induced Explosion in High Strength Concrete.
- Uniaxial Stress-Strain Curves of High Strength Concrete.
- The Strength of Overlapped Deformed Tensile Reinforcement Splices in High Strength Concrete.

The thesis has been carried out at the Department of Structural Engineering, Technical University of Denmark under the supervision of Lecturer, M.Sc. Erik Skettrup, Lecturer, Dr. Herbert Krenchel and Professor Emeritus, Dr. Troels Brøndum-Nielsen.

I wish to express my sincere thanks to the staff of the Department of Structural Engineering for all their help in the completion of this report.

Finally, I wish to acknowledge the financial support of the Danish Technical Research Council Contract No.: FTU 5.17.3.6.11 without which it had not been possible to carry out this research.

## ABSTRACT

The thesis deals with the following four investigations:

- Heat-Induced Explosion in High Strength Concrete.
- Uniaxial Stress-Strain Curves of High Strength Concrete.
- Design Proposal for High Strength Concrete Sections Subjected to Flexural and Axial Loads.
- The Strength of Overlapped Deformed Tensile Reinforcement Splices in High Strength Concrete.

The thesis consist of four sepearate reports. A short summary of these is given below.

### Heat-Induced Explosions in High Strength Concrete.

This report contains the result and description of a series of tests which have been carried out in order to evaluate the explosion risk of heat induced high strength concrete as compared to normal strength concrete.

The tests were carried out with concrete test specimens shaped as  $\emptyset 100 \times 200$  mm cylinders with a compressive strength in the range from 30 MPa to 90 MPa. The cylinders were cured in two different ways:

- a: 7 days in water followed by 21 days in laboratory atmosphere (  $20^{\circ}$  C and 60 % RH ).

b: 7 days in water followed by 21 days sealed with plastic aluminum foil.

A total of 36 concrete cylinders were heated in an electrical oven at a heating rate of  $2.5^{\circ}$  C per min. until reaching a temperature of  $600^{\circ}$  C. After 2 hours at this temperature the cylinders were cooled at a rate of up to  $1^{\circ}$  C per min.

The tests show that the explosion risk depends on the curing conditions and that the explosion risk in the case of high strength concrete is not higher than for normal strength concrete especially for concrete cured under condition a.

#### Uniaxial Stress-Strain Curves of High Strength Concrete.

This report describes a special test-rig developed in order to obtain the ascending as well as the descending part of uniaxial stress-strain curves. Test results is reported from test series where the complete stress-strain curve is determined for concrete with compressive strength in the range from 40 MPa to 92 MPa.

The test results show that the ascending part of the uniaxial stress-strain curves are more linear and steeper for high strength concrete when compared to normal strength concrete and that the descending branch becomes steeper the higher the strength level.

The inclination of the ascending part of the obtained uniaxial stress-strain curves for high strength concrete is steeper and the strain at peak stress is less when compared to results from USA and Norway. The declination of the descending part seems less when compared to the results from Norway and only slightly steeper when compared to results from USA.

Design Proposal for High Strength Concrete Sections Subjected to Flexural and Axial Loads.

In this report an investigation is carried out of the consequences when predicting the ultimate capacity of reinforced high strength concrete sections subjected to pure bending or combined bending and axial load by extrapolating DS 411 to the compressive strength level of 90 MPa. The investigation is based on calculated results using obtained knowledge of the complete uniaxial stress-strain curves for concrete and applying nonlinear computerized methods.

The investigation show that extrapolation of DS 411 overestimates the ultimate capacity of reinforced high strength concrete sections when subjected to pure bending with as much as 33 %, while DS 411 in the case of sections subjected to combined bending and axial load overestimates the ultimate capacity with as much as 39 %.

A design proposal is suggested for calculating the ultimate capacity of high strength concrete sections subjected to pure bending or combined bending and axial load. The design proposal is based on the same principles as DS 411 and the results from the nonlinear calculations using the knowledge of the complete uniaxial stress-strain curves as mentioned above.

The curvature ductility of single reinforced high strength concrete sections compared to normal strength concrete sections is also investigated on the basis of results from the nonlinear calculations. The investigation show that the ductility of high strength concrete sections is less than the ductility of normal strength concrete sections regardless of the reinforcement degree and that it can be reduced to as much as 78 %.

## The Strength of Overlapped Deformed Tensile Reinforcement Splices in High Strength Concrete.

This report describes a test series carried out in order to evaluate the strength of overlapped tensile splices in high strength concrete and the anchorage strength of deformed bars in pull-out test specimens similar to that of DS 2082.

The influence of concrete compressive strength, splitting strength and fracture energy,  $G_f$ , on the strength of overlapped tensile splices is evaluated on the basis of 22 tests. The test indicate that the fracture energy of concrete appears to be a more governing property to the strength of splices than the compressive strength and splitting strength.

The results from the tests with overlapped splices is compared to the Danish Code of Practice for the use of Concrete, DS 411. The comparison show that extrapolating DS 411 for the design of overlapped splices in high strength concrete will yield more conservative results than in the case of normal strength concrete.

The results from the tests with overlapped splices have also been compared to estimated values from a theoretical model developed at the Department of Structural Engineering by B. S. Andreasen. The model is based on the theory of plasticity and tests with concrete in the normal strength range. The comparison show that the model developed by Andreasen overestimates the strength of overlapped splices for high strength concrete. A modification to the  $\nu$ -expression used in the model is suggested, yielding more acceptable deviations from the test results.

Estimated values from an empirical formula developed by Orangun et al. is compared to the results from the tests with overlapped splices. The comparison show that the empirical formula overestimates the strength of overlapped splices in high strength concrete.



The influence of concrete compressive strength, splitting strength and fracture energy,  $G_F$ , on the anchorage strength of deformed bars in pull-out test specimens is evaluated on the basis of 84 tests. No clear conclusion could be made from the tests regarding which property were the most governing on the anchorage strength.

A model is suggested for calculating the anchorage strength of deformed bars in pull-out test specimens similar to that of DS 2082. The model is based on the theory of plasticity as well as the experimental results and the principles used by Andreassen in his model for estimating the strength of overlapped splices.

The results from the tests with overlapped splices and pull-out tests are compared. The comparison indicates that the anchorage strength from the pull-out tests are considerably larger than the strength from overlapped splices regardless of the concrete compressive strength level. The reason for this is partly the surrounding spiral reinforcement in the pull-out test specimen which confine the concrete around the anchored bar and that the failure mechanism is completely different from that of overlapped splices.

## RESUME

Afhandlingen omhandler følgende undersøgelser af højstyrkebeton:

- Heat-Induced Explosion in High Strength Concrete.
- Uniaxial Stress-Strain Curves of High Strength Concrete.
- Design Proposal for High Strength Concrete Sections Subjected to Flexural and Axial Loads.
- The Strength of Overlapped Deformed Tensile Reinforcement Splices in High Strength Concrete.

Afhandlingen foreligger som fire separate rapporter over undersøgelserne og er kort resumeret nedenfor.

### Heat-Induced Explosion in High Strength Concrete.

Denne rapport indeholder resultater og beskrivelse af en forsøgsrække udført med det formål, at undersøge explosionsrisikoen af varmpåvirket højstyrkebeton i forhold til normalstyrkebeton.

Undersøgelsen omfatter betonprøvelegemer formet som  $\varnothing 100 \times 200$  mm cylindre med en trykstyrke i intervallet 30 - 90 MPa, som er hærdnet på to forskellige måder :

- a: 7 dage i vand efterfulgt af 21 dage i laboratoriet ved  $20^{\circ}$  C og 60 % RH.

b: 7 dage i vand efterfulgt af 21 dage forseglet med plastik og aluminiums folie.

Ialt 36 betoncylindre blev opvarmet i en elektrisk ovn med en opvarmningshastighed på  $2.5^{\circ}$  C pr. min. op til  $600^{\circ}$  C. Efter 2 timer ved  $600^{\circ}$  C blev cylindrene nedkølet med en hastighed på maksimalt  $1^{\circ}$  C pr. min.

Forsøgene viste, at explosionsrisikoen afhænger af hærdningsforholdene, samt at risikoen for højstyrkebeton ikke er væsentligt højere end for normalstyrkebeton, specielt når disse hærdes som under a.

#### Uniaxial Stress-Strain Curves of High Strength Concrete.

Rapporten beskriver en specielt udviklet forsøgsopstilling, som muliggør bestemmelse af den stigende og faldende del af enaksede betonarbejdskurver.

Rapporten indeholder derudover resultater fra forsøgsrækker, hvor hele den enaksede arbejdskurve er bestemt for beton med trykstyrker i intervallet 40 - 92 MPa. De bestemte enaksede arbejdskurver af højstyrkebeton udviser i forhold til normalstyrkebeton et mere lineært og stejlere forløb af den nedadgående del.

De opnåede arbejdskurver for højstyrkebeton udviser sammenlignet med tilsvarende arbejdskurver fra USA og Norge et stejlere forløb af den stigende del af arbejdskurven, og en mindre tøjning ved maksimal spænding, mens den nedadgående del er mindre stejl sammenlignet med de norske resultater og stejlere sammenlignet med de amerikanske resultater.

## Design Proposal for High Strength Concrete Sections Subjected to Flexural and Axial Loads.

I denne rapport vurderes om beregningsmetoden i DS 411 til bestemmelse af betontværsnits bæreevne, påvirket til ren bøjning eller kombineret bøjning og normalkraft, kan ekstrapoleres til betonstyrker i intervallet 50 -90 MPa. Vurderingen er baseret på resultaterne fra en ulineær beregningsmodel, hvor der indgår både den stigende og den faldende del af eksperimentelt bestemte enaksede betonarbejdskurver fra en tidligere undersøgelse.

Bestemmes højstyrkebetontværsnits bæreevne ved ekstrapolering af DS 411 kan bæreevnen af tværsnit med balanceret armeringsgrad påvirket til ren bøjning overvurderes med op til 33 % i forhold til resultaterne fra den ulineære beregning, mens bæreevnen af tværsnit påvirket til kombineret bøjning og normalkraft kan overvurderes med op til 39 %.

Et beregningsforslag er derfor udarbejdet til bestemmelse af højstyrkebetontværsnits bæreevne påvirket til ren bøjning eller kombineret bøjning med normalkraft. Forslaget er baseret på de samme principper som DS 411 og resultater fra den ulineære beregningsmodel.

Endvidere er duktiliteten af højstyrkebetontværsnit vurderet i forhold til normalstyrkebetontværsnit på baggrund af resultaterne fra den ulineære beregningsmodel.

Resultaterne indikerer, at duktiliteten af højstyrkebetontværsnit er mindre uanset armeringsgraden af tværsnittet og kan forminskes ned til 78 % af tilsvarende normalbetontværsnit.

## The Strength of Overlapped Deformed Tensile Reinforcement Splices in High Strength Concrete.

I denne rapport beskrives for både højstyrkebeton og normalstyrkebeton en eksperimentel behandling af overlappingsstøds bæreevne samt bæreevnen af forkammet armering forankret i prøvelegemer meget lig prøvelegemet efter Dansk Standard DS 2082.

Inflydelsen af betons trykstyrke, spaltetrækstyrke og brudenergi,  $G_F$ , på bæreevnen af overlappingsstød er undersøgt på basis af 22 forsøg. Undersøgelsen viser, at betons brudenergi  $G_F$  har større indflydelse på bæreevnen af overlappingsstød end betons trykstyrke og spaltetrækstyrke.

Der er foretaget en undersøgelse af muligheden for, at ekstrapolere beregningsmodellen i DS 411 til beregning af nødvendig overlappingslængde af stød til betonstyrker i intervallet 50 - 90 MPa. Denne undersøgelse viser, at DS 411 ved ekstrapolering giver mere konservative resultater af nødvendig overlappingslængde for højstyrkebeton end for normalstyrkebeton.

Resultaterne af forsøgene med overlappingsstød er sammenlignet med resultater fra en beregningsmodel udviklet på Afdelingen for Bærende Konstruktioner af B. S. Andreasen. Modellen der baseres på plasticitetsteorien og forsøg primært med betontrykstyrker i intervallet 6 - 50 MPa, overvurderer bæreevnen af overlappingsstød i højstyrkebeton. Et forslag til et andet  $\nu$ -udtryk til beregningsmodellen er derfor udarbejdet.

Derudover er forsøgsresultaterne med overlappingsstød sammenlignet med resultater fra en empirisk formel udviklet af Orangun et al, der viser at den empiriske formel overvurderer bæreevnen af overlappingsstød i højstyrkebeton.

Inflydelsen af betons trykstyrke, spaltetrækstyrke og brudenergi  $G_F$  på bæreevnen af forankret armering i prøvelegemer meget lig prøvelegemer efter DS 2082 er undersøgt på basis af 84 forsøg. Det har ikke på baggrund af disse forsøg været muligt at fastslå hvilken af ovennævnte parametre, der har størst indflydelse på bæreevnen.

Et forslag til en beregningsmodel er udviklet til beregning af forkammet armerings bæreevne i prøvelegemer meget lig prøvelegemet i DS 2082. Beregningsmodellen er baseret på plasticitetsteorien og de gennemførte forsøg samt principperne anvendt af Andreasen i beregningsmodellen for bæreevnen af overlappingsstød.

En sammenligning mellem de eksperimentelt fundne bæreevner af overlappingsstød og forankring af forkammet armering viser, at sidstnævnte generelt har højere bæreevne. Dette kan skyldes, at spiralarmeringen omslutter betonen hvori armeringsjernet er forankret samt, at brudmekanismen er forskellig fra brudmekanismen i overlappingsstød.

<u>CONTENT</u>	PAGE
PREFACE .....	i
ABSTRACT .....	ii
RESUME .....	vii
LIST OF TABLES .....	xiv
LIST OF FIGURES .....	xvi
NOTATIONS .....	xxv
1. INTRODUCTION .....	1
1.1 Purpose of this investigation .....	3
1.2 Format .....	3
2. UNIAXIAL STRESS-STRAIN CURVES .....	4
2.1 Introduction .....	4
2.2 Establishing the Stress-Strain Curves .....	4
2.3 Mathematical Representation of the Stress-Strain Curves .....	6
3. NONLINEAR MODEL FOR CROSS-SECTIONAL ANALYSIS .....	10
3.1 Introduction .....	10
3.2 Assumptions in the Nonlinear Model .....	10
3.3 Technique of Analysis .....	13
4. DESIGN PROPOSAL .....	18
4.1 Introduction .....	18
4.2 Ultimate Moment Capacity .....	18
4.3 Ultimate Capacity of Combined Bending and Axial Load .....	19

	PAGE
5. DS 411 AND THE DESIGN PROPOSAL COMPARED	
TO THE NONLINEAR MODEL .....	21
5.1 Introduction .....	21
5.2 Ultimate Moment Capacity without	
Compression Reinforcement .....	21
5.3 Ultimate Moment Capacity with	
Compression Reinforcement .....	23
5.4 Ultimate Capacity of Combined Bending	
and Axial Load .....	24
6. DUCTILITY INDEX AND ULTIMATE PLASTIC ROTATION .....	27
6.1 Introduction .....	27
6.2 Definitions .....	27
6.3 Ductility .....	29
6.4 Ultimate Plastic Rotation .....	31
7. CONCLUSION .....	33
8. REFERENCES .....	36
9. TABLES .....	40
10 FIGURES .....	49



**LIST OF TABLES**

**PAGE**

2.1	Average values of the three key points and the constants in the mathematical representation .....	40
4.1	Values of $\eta$ , $\beta$ and $\epsilon_{cu}$ for concrete compressive strengths, $f_c$ , in the range from 40 to 90 MPa .....	41
5.1	Maximum deviations of the proposal and DS 411 when compared to the nonlinear model, assuming pure bending and only tensional reinforcement .....	41
5.2	Maximum deviation of DS 411 and the proposal when compared to the nonlinear model, assuming pure bending and sections containing compressive reinforcement .....	42
5.3	Maximum deviation of $\mu-\nu$ relationships estimated from DS 411 and the proposal when compared to the nonlinear results in cases of cross-sections with concrete on a 40 MPa level .....	43
5.4	Maximum deviation of $\mu-\nu$ relationships estimated from DS 411 and the proposal when compared to the nonlinear results in cases of cross-sections with concrete on a 50 MPa level .....	44
5.5	Maximum deviation of $\mu-\nu$ relationships estimated from DS 411 and the proposal when compared to the nonlinear results in cases of cross-sections with concrete on a 60 MPa level .....	45
5.6	Maximum deviation of $\mu-\nu$ relationships estimated from DS 411 and the proposal when compared to the nonlinear results in cases of cross-sections with concrete on a 70 MPa level .....	46

5.7	Maximum deviation of $\mu$ - $\nu$ relationships estimated from DS 411 and the proposal when compared to the nonlinear results in cases of cross-sections with concrete on a 80 MPa level .....	47
5.8	Maximum deviation of $\mu$ - $\nu$ relationships estimated from DS 411 and the proposal when compared to the nonlinear results in cases of cross-sections with concrete on a 90 MPa level .....	48

<u>LIST OF FIGURES</u>	PAGE
2.1 The test rig .....	49
2.2 Details of the test rig .....	49
2.3 Photo of the test rig .....	50
2.4 Examples of obtained stress-strain curves .....	51
2.5 An example of the mathematical fit to experimental results from normal strength concrete .....	51
2.6 Comparison between the first proposed expression and the suggested practical proposal, in the case of high strength concrete on a 90 MPa level .....	52
2.7 Comparison between the first proposed expression and the suggested practical proposal, in the case of normal strength concrete on a 40 MPa level .....	52
3.1 Bilinear stress-strain relationship for the rein- forcement steel used in the nonlinear analysis .....	53
3.2 Cross-section subjected to pure bending in the non- linear model .....	53
3.3 An example of moment-curvature curve .....	54
3.4 Cross-section subjected to exentric axial load in the nonlinear model .....	54

	PAGE
4.1 Cross-section subjected to pure bending in the design proposal .....	55
4.2 Suggested interaction diagram when the section is underreinforced .....	56
4.3 Suggested interaction diagram when the section is balanced reinforced or overreinforced .....	56
5.1 $\mu$ - $\omega$ relationship of DS 411, the proposal and the non-linear model in the case of pure bending only tensional reinforcement and concrete compressive strength on a 40 MPa level .....	57
5.2 $\mu$ - $\omega$ relationship of DS 411, the proposal and the non-linear model in the case of pure bending only tensional reinforcement and concrete compressive strength on a 50 MPa level .....	57
5.3 $\mu$ - $\omega$ relationship of DS 411, the proposal and the non-linear model in the case of pure bending only tensional reinforcement and concrete compressive strength on a 60 MPa level .....	58
5.4 $\mu$ - $\omega$ relationship of DS 411, the proposal and the non-linear model in the case of pure bending only tensional reinforcement and concrete compressive strength on a 70 MPa level .....	58
5.5 $\mu$ - $\omega$ relationship of DS 411, the proposal and the non-linear model in the case of pure bending only tensional reinforcement and concrete compressive strength on a 80 MPa level .....	59

	PAGE
5.6 $\mu$ - $\omega$ relationship of DS 411, the proposal and the non-linear model in the case of pure bending only tensional reinforcement and concrete compressive strength on a 90 MPa level .....	59
5.7 Balanced mechanical reinforcement ratio as a function of the concrete compressive strength .....	60
5.8 $\mu$ - $\omega$ relationship of the Danish Code, DS 411, the proposal and the nonlinear model. The sections are subjected to pure bending and containing compressive steel ratios 0.2, 0.4 and 0.6 of the tensional steel amount. The concrete compressive strength of the section is on a 40 MPa level .....	61
5.9 $\mu$ - $\omega$ relationship of the Danish Code, DS 411, the proposal and the nonlinear model. The sections are subjected to pure bending and containing compressive steel ratios 0.2, 0.4 and 0.6 of the tensional steel amount. The concrete compressive strength of the section is on a 50 MPa level .....	62
5.10 $\mu$ - $\omega$ relationship of the Danish Code, DS 411, the proposal and the nonlinear model. The sections are subjected to pure bending and containing compressive steel ratios 0.2, 0.4 and 0.6 of the tensional steel amount. The concrete compressive strength of the section is on a 60 MPa level .....	63
5.11 $\mu$ - $\omega$ relationship of the Danish Code, DS 411, the proposal and the nonlinear model. The sections are subjected to pure bending and containing compressive steel ratios 0.2, 0.4 and 0.6 of the tensional steel amount. The concrete compressive strength of the section is on a 70 MPa level .....	64

5.12 $\mu$ - $\omega$ relationship of the Danish Code, DS 411, the proposal and the nonlinear model. The sections are subjected to pure bending and containing compressive steel ratios 0.2, 0.4 and 0.6 of the tensional steel amount. The concrete compressive strength of the section is on a 80 MPa level .....	65
5.13 $\mu$ - $\omega$ relationship of the Danish Code, DS 411, the proposal and the nonlinear model. The sections are subjected to pure bending and containing compressive steel ratios 0.2, 0.4 and 0.6 of the tensional steel amount. The concrete compressive strength of the section is on a 90 MPa level .....	66
5.14 Balanced mechanical tensional reinforcement ratio as a function of the compressive steel ratio in the case of sections subjected to pure bending and concrete compressive strength of the sections on a 40 MPa level .....	67
5.15 Balanced mechanical tensional reinforcement ratio as a function of the compressive steel ratio in the case of sections subjected to pure bending and concrete compressive strength of the sections on a 50 MPa level .....	67
5.16 Balanced mechanical tensional reinforcement ratio as a function of the compressive steel ratio in the case of sections subjected to pure bending and concrete compressive strength of the sections on a 60 MPa level .....	68
5.17 Balanced mechanical tensional reinforcement ratio as a function of the compressive steel ratio in the case of sections subjected to pure bending and concrete compressive strength of the sections on a 70 MPa level .....	68

- 5.18 Balanced mechanical tensional reinforcement ratio as a function of the compressive steel ratio in the case of sections subjected to pure bending and concrete compressive strength of the sections on a 80 MPa level ..... 69
- 5.19 Balanced mechanical tensional reinforcement ratio as a function of the compressive steel ratio in the case of sections subjected to pure bending and concrete compressive strength of the sections on a 90 MPa level ..... 69
- 5.20  $\mu$ - $\nu$  relationships of the Danish Code, DS 411, the proposal and the nonlinear model. The concrete compressive strength of the section is on a 40 MPa level. The section has a mechanical tensional steel ratio  $\omega = 0.5 \times \omega_{bal}$  and mechanical compressive steel ratio  $\omega_c = 0$ ,  $\omega_c = 0.5 \times \omega$  and  $\omega_c = \omega$  ..... 70
- 5.21  $\mu$ - $\nu$  relationships of the Danish Code, DS 411, the proposal and the nonlinear model. The concrete compressive strength of the section is on a 40 MPa level. The section has a mechanical tensional steel ratio  $\omega = 1.0 \times \omega_{bal}$  and mechanical compressive steel ratio  $\omega_c = 0$ ,  $\omega_c = 0.5 \times \omega$  and  $\omega_c = \omega$  ..... 71
- 5.22  $\mu$ - $\nu$  relationships of the Danish Code, DS 411, the proposal and the nonlinear model. The concrete compressive strength of the section is on a 40 MPa level. The section has a mechanical tensional steel ratio  $\omega = 1.5 \times \omega_{bal}$  and mechanical compressive steel ratio  $\omega_c = 0$ ,  $\omega_c = 0.5 \times \omega$  and  $\omega_c = \omega$  ..... 72

- 5.23  $\mu$ - $\nu$  relationships of the Danish Code, DS 411, the proposal and the nonlinear model. The concrete compressive strength of the section is on a 50 MPa level. The section has a mechanical tensional steel ratio  $\omega = 0.5 \times \omega_{bal}$  and mechanical compressive steel ratio  $\omega_c = 0$ ,  $\omega_c = 0.5 \times \omega$  and  $\omega_c = \omega$  ..... 73
- 5.24  $\mu$ - $\nu$  relationships of the Danish Code, DS 411, the proposal and the nonlinear model. The concrete compressive strength of the section is on a 50 MPa level. The section has a mechanical tensional steel ratio  $\omega = 1.0 \times \omega_{bal}$  and mechanical compressive steel ratio  $\omega_c = 0$ ,  $\omega_c = 0.5 \times \omega$  and  $\omega_c = \omega$  ..... 74
- 5.25  $\mu$ - $\nu$  relationships of the Danish Code, DS 411, the proposal and the nonlinear model. The concrete compressive strength of the section is on a 50 MPa level. The section has a mechanical tensional steel ratio  $\omega = 1.5 \times \omega_{bal}$  and mechanical compressive steel ratio  $\omega_c = 0$ ,  $\omega_c = 0.5 \times \omega$  and  $\omega_c = \omega$  ..... 75
- 5.26  $\mu$ - $\nu$  relationships of the Danish Code, DS 411, the proposal and the nonlinear model. The concrete compressive strength of the section is on a 60 MPa level. The section has a mechanical tensional steel ratio  $\omega = 0.5 \times \omega_{bal}$  and mechanical compressive steel ratio  $\omega_c = 0$ ,  $\omega_c = 0.5 \times \omega$  and  $\omega_c = \omega$  ..... 76
- 5.27  $\mu$ - $\nu$  relationships of the Danish Code, DS 411, the proposal and the nonlinear model. The concrete compressive strength of the section is on a 60 MPa level. The section has a mechanical tensional steel ratio  $\omega = 1.0 \times \omega_{bal}$  and mechanical compressive steel ratio  $\omega_c = 0$ ,  $\omega_c = 0.5 \times \omega$  and  $\omega_c = \omega$  ..... 77



- 5.28  $\mu$ - $\nu$  relationships of the Danish Code, DS 411, the proposal and the nonlinear model. The concrete compressive strength of the section is on a 60 MPa level. The section has a mechanical tensional steel ratio  $\omega = 1.5 \times \omega_{bal}$  and mechanical compressive steel ratio  $\omega_c = 0$ ,  $\omega_c = 0.5 \times \omega$  and  $\omega_c = \omega$  ..... 78
- 5.29  $\mu$ - $\nu$  relationships of the Danish Code, DS 411, the proposal and the nonlinear model. The concrete compressive strength of the section is on a 70 MPa level. The section has a mechanical tensional steel ratio  $\omega = 0.5 \times \omega_{bal}$  and mechanical compressive steel ratio  $\omega_c = 0$ ,  $\omega_c = 0.5 \times \omega$  and  $\omega_c = \omega$  ..... 79
- 5.30  $\mu$ - $\nu$  relationships of the Danish Code, DS 411, the proposal and the nonlinear model. The concrete compressive strength of the section is on a 70 MPa level. The section has a mechanical tensional steel ratio  $\omega = 1.0 \times \omega_{bal}$  and mechanical compressive steel ratio  $\omega_c = 0$ ,  $\omega_c = 0.5 \times \omega$  and  $\omega_c = \omega$  ..... 80
- 5.31  $\mu$ - $\nu$  relationships of the Danish Code, DS 411, the proposal and the nonlinear model. The concrete compressive strength of the section is on a 70 MPa level. The section has a mechanical tensional steel ratio  $\omega = 1.5 \times \omega_{bal}$  and mechanical compressive steel ratio  $\omega_c = 0$ ,  $\omega_c = 0.5 \times \omega$  and  $\omega_c = \omega$  ..... 81
- 5.32  $\mu$ - $\nu$  relationships of the Danish Code, DS 411, the proposal and the nonlinear model. The concrete compressive strength of the section is on a 80 MPa level. The section has a mechanical tensional steel ratio  $\omega = 0.5 \times \omega_{bal}$  and mechanical compressive steel ratio  $\omega_c = 0$ ,  $\omega_c = 0.5 \times \omega$  and  $\omega_c = \omega$  ..... 82

- 5.33  $\mu$ - $\nu$  relationships of the Danish Code, DS 411, the proposal and the nonlinear model. The concrete compressive strength of the section is on a 80 MPa level. The section has a mechanical tensional steel ratio  $\omega = 1.0 \times \omega_{bal}$  and mechanical compressive steel ratio  $\omega_c = 0$ ,  $\omega_c = 0.5 \times \omega$  and  $\omega_c = \omega$  ..... 83
- 5.34  $\mu$ - $\nu$  relationships of the Danish Code, DS 411, the proposal and the nonlinear model. The concrete compressive strength of the section is on a 80 MPa level. The section has a mechanical tensional steel ratio  $\omega = 0.5 \times \omega_{bal}$  and mechanical compressive steel ratio  $\omega_c = 0$ ,  $\omega_c = 0.5 \times \omega$  and  $\omega_c = \omega$  ..... 84
- 5.35  $\mu$ - $\nu$  relationships of the Danish Code, DS 411, the proposal and the nonlinear model. The concrete compressive strength of the section is on a 90 MPa level. The section has a mechanical tensional steel ratio  $\omega = 0.5 \times \omega_{bal}$  and mechanical compressive steel ratio  $\omega_c = 0$ ,  $\omega_c = 0.5 \times \omega$  and  $\omega_c = \omega$  ..... 85
- 5.36  $\mu$ - $\nu$  relationships of the Danish Code, DS 411, the proposal and the nonlinear model. The concrete compressive strength of the section is on a 90 MPa level. The section has a mechanical tensional steel ratio  $\omega = 1.0 \times \omega_{bal}$  and mechanical compressive steel ratio  $\omega_c = 0$ ,  $\omega_c = 0.5 \times \omega$  and  $\omega_c = \omega$  ..... 86
- 5.37  $\mu$ - $\nu$  relationships of the Danish Code, DS 411, the proposal and the nonlinear model. The concrete compressive strength of the section is on a 90 MPa level. The section has a mechanical tensional steel ratio  $\omega = 1.5 \times \omega_{bal}$  and mechanical compressive steel ratio  $\omega_c = 0$ ,  $\omega_c = 0.5 \times \omega$  and  $\omega_c = \omega$  ..... 87

	PAGE
6.1 Definition of ultimate curvature, $\kappa_u$ , and curvature ductility index, $\delta_c$ .....	88
6.2 Curvature ductility index, $\delta_c$ , as a function of relatively reinforcement ratio, $\omega/\omega_{bal}$ .....	89
6.3 Relatively curvature ductility index, $\delta_c/\delta_{c,40 \text{ MPa}}$ as function of relatively reinforcement ratio $\omega/\omega_{bal}$ . $\delta_{c,40 \text{ MPa}}$ is the curvature ductility in the case of sections with concrete having compressive strength in a 40 MPa level .....	90
6.4 Improvement of curvature ductility index by adding reinforcement in the compression zone of 90 MPa high strength concrete sections .....	90
6.5 Ultimate plasticity rotation, $\theta_{pl}$ in radians, as a function of $\omega/\omega_{bal}$ .....	91

## NOTATIONS

The most commonly used symbols are listed below. Exceptions from the list can appear, but this will be mentioned in the text in connection to actual symbol.

$b$	Width of beam section.
$c_1$	Vertical distance from the top of the beam to center of the compressive reinforcement.
$h$	Total depth of beam section.
$h_c$	Depth of compression zone.
$h_{ef}$	Depth to the center of the tensile reinforcement.
$k$	Constant used in a mathematical expression for the descending part of the uniaxial stress-strain curves.
$\gamma$	Dimensionless stress.
$x$	Dimensionless strain.
$A_a, B_a, C_a, D_a$	Constants used in a mathematical expression for the ascending part of uniaxial stress-strain curves.
$A_d, B_d, C_d, D_d$	Constants used in a mathematical expression for the descending part of uniaxial stress-strain curves.
$A_{sc}$	Cross-sectional area of the compressive reinforcement
$A_{st}$	Cross-sectional area of the tensile reinforcement
$E_c$	Secant modulus of elasticity determined from the origo of the uniaxial stress-strain curves to 45 % of the peak stress.
$E_{co}$	Secant modulus of elasticity determined from the origo of uniaxial stress-strain curves to the peak stress.
$F_c$	Total compressive load in the concrete.
$F_{sc}$	Total load in the compressive reinforcement
$F_{st}$	Total load in the tensile reinforcement
$L_{pl}$	The plasticity length of the plastic hinge.
$M$	Bending moment.
$N$	Normal force.

$\alpha$	Constant used in a mathematical expression for uniaxial stress-strain curves.
$\beta$	The ratio of the stress in the equivalent rectangular stress distribution to the compressive strength.
$\delta_c$	Curvature ductility index.
$\delta_d$	Displacement ductility index.
$\epsilon_c$	Concrete compressive strain.
$\epsilon_{co}$	Concrete compressive strain at peak stress.
$\epsilon_{cu}$	Ultimate compressive strain of concrete.
$\epsilon_{sc}$	Compressive steel strain.
$\epsilon_{st}$	Tensile steel strain.
$\kappa_y$	Sectional curvature at first yield of the tensile steel
$\kappa_u$	Sectional curvature at ultimate load.
$\eta$	The ratio of the depth of the equivalent compressive stress block to the depth of the actual one.
$\theta_{pl}$	Ultimate plastic rotation.
$\mu$	Dimensionless moment.
$\nu$	Dimensionless normal force.
$\sigma_c$	Concrete stress.
$\sigma_{co}$	Concrete peak stress.
$\sigma_{st}$	Tensile steel stress.
$\sigma_{sc}$	Compressive steel stress.
$\omega$	Mechanical ratio of tensile reinforcement.
$\omega_c$	Mechanical ratio of compressive reinforcement.
$\omega_{bal}$	Balanced mechanical reinforcement ratio of sections subjected to pure bending and without compressive reinforcement.

## 1. INTRODUCTION

The ultimate strength of reinforced concrete members subjected to flexure and axial loads can be predicted using an equivalent rectangular stress distribution on the concrete compressive zone. This is the case in the Danish code DS 411 [1]. The design requires the knowledge of three parameters:

$\beta$  : The ratio of the stress in the equivalent rectangular stress distribution to the compressive strength. In DS 411  $\beta$  is set to 1.0.

$\eta$  : The ratio of the depth of the equivalent compressive block to the depth of the actual one. In DS 411  $\eta$  is set to 0.8.

$\epsilon_{cu}$  : Ultimate compressive strain of concrete. In DS 411  $\epsilon_{cu}$  is set to 0.0035.

In addition the code presuppose, that the structure has adequate yield capacity, when the theory of plasticity is used for the determination of stress results, i.e. yielding in the reinforcement will develop to a sufficient extent before other forms of failure, such as instability, terminate a ductile failure in progress. In other words the code requires, that the ratio of the tensile reinforcement must be less than the ratio which produces simultaneous crushing of concrete in compression and yielding of steel in tension.

The values of these parameters and the validity of the code are based on extensive tests on reinforced concrete columns and beams using concretes with compressive strengths of less than 50 MPa. High strength concretes are, however, currently being used and a modification of the preceding parameters is necessary for such high strength concretes.

One approach to develop parameters defining the high strength concrete compression zone at the ultimate strength of reinforced

members is to test members made of high strength concretes. However, since the properties of the concrete compression zone in the ultimate stage not only depend on the concrete compressive strength, but also on the stress-strain curve and the amount of reinforcement, and the relative amounts of flexure and axial loads applied to the members, the experimental program would have to be very extensive.

Another approach is to calculate the ultimate strength of structural members using a knowledge of the stress-strain curves for concrete and steel and applying nonlinear computerized methods. The values related to the concrete compression zone could then be predicted by analytic procedures for a wide variety of design situations.

Knowledge of stress-strain curves for high strength concrete and normal strength concrete, produced with Danish materials were established at the Department of Structural Engineering in a previous investigation, Olsen [2]. A special test-rig were developed capable of recording the ascending as well as the descending branch of uniaxial stress-strain curves both for high strength and normal strength concrete.

Stress-strain curves for four types of concrete having compressive strengths as follows were established:

- 1) High strength concrete on a 90 MPa level
- 2) High strength concrete on a 70 MPa level
- 3) Normal strength concrete on a 50 MPa level
- 4) Normal strength concrete on a 40 MPa level.

Using an approach of nonlinear computerized analysis techniques, it is then possible to rationally predict the ultimate capacity and sectional ductility of structural members when given their cross-sectional properties, material properties and load conditions.

## 1.1 Purpose of the Investigation.

The main purpose of this investigation is to suggest a simple design proposal capable of predicting the ultimate capacity of high and normal strength concrete cross-sections subjected to pure bending or combined bending and axial loads. Furthermore it is the purpose to describe the consequences, when using the Danish Code DS 411 to predict the ultimate capacity of high strength concrete sections.

## 1.2 Format

The next chapter gives a review of how the uniaxial stress-strain curves were established and gives the mathematical representation of the curves used in the nonlinear model. In chapter 3 the nonlinear model and its assumptions are described followed by a description of the suggested design proposal in chapter 4. The Danish Code DS 411 and the suggested design proposal is compared to the nonlinear model in chapter 5. The ductility of structural members produced with high strength concrete is described in chapter 6.



## 2. UNIAXIAL STRESS-STRAIN CURVES

### 2.1 Introduction.

When using the uniaxial stress-strain curves for concrete and applying computerized nonlinear techniques to predict the ultimate capacity of concrete structural members it is necessary to obtain accurate knowledge of not only the ascending portion of the stress-strain curve but also the descending portion. This knowledge is necessary since part of the strains in the concrete compressive zone at the ultimate limit state usually is in the descending portion of the stress-strain curve.

Data regarding the complete stress-strain curve of high strength concrete produced with Danish materials is not previously obtained. It was therefore necessary to develop a special test-rig capable of recording both the ascending and the descending branch of uniaxial stress-strain curves from concretes and to conduct several test series involving high and normal strength concretes.

The following sections give a brief review of the test-rig used to establish data concerning the stress-strain curves of two high and two normal strength concretes. Furthermore the mathematical representations of the stress-strain curves which is used in the computerized nonlinear analysis is given. A more detailed description of the test-rig and the experimental results can be found in Olsen [2].

### 2.2 Establishing the Stress-Strain Curves.

One of the reasons, why there is insufficient experimental information on the shape of the stress-strain curve beyond the peak stress, is the difficulty in experimentally establishing the descending portion of the curve. Many testing machines used for standard compression test apply increasing loads rather than increasing deformation. This results in an uncontrolled sudden failure immediately after the peak load.

Several investigators have developed techniques to obtain the complete stress-strain curves of concretes [3]-[6]. Some of these techniques are very costly and require testing machines which may not be available in a normal laboratory or require extensive modifications to a standard testing machine.

In the investigation conducted at the Department of Structural Engineering a simple technique was developed to obtain the complete stress-strain curve of high strength concrete produced with Danish materials. The test rig consists of 3 parallel steel columns and a cylindrical steel block placed centrally between them upon which the cylindrical concrete specimen is placed. The loading of the concrete specimen takes place in parallel with the 3 steel columns. Fig. 2.1 and 2.2 show the test rig and its dimension. Fig. 2.3 is a photo of the test rig.

Capping both ends of the concrete cylinder with Technovit 2060 prior to testing ensured that the machine head would apply load simultaneously to the steel columns and the concrete cylinder. The load from the testing machine was applied continuously so that the strain rate on the concrete cylinder was approximately 2 microstrain/second at the ascending part of the stress-strain curves. As a consequence of the expansion of the cylindrical steel block upon which the concrete specimen is placed, the strain rate varies at the descending part of the stress strain curves depending on the brittleness of the concrete. In the test conducted at the Department, this strain rate was recorded to a maximum of 35 microstrain/second.

During loading the strains in the 3 steel columns and steel cylindrical block were measured with 6 mm long strain gauges in full bridge configuration. These gauges gave not only the strain in the cylindrical concrete specimen but also the stress in the specimen, since the cylindrical steel block were calibrated prior to the tests. Furthermore, 4 strain gauges 85 mm long were placed directly on the generatrices of the concrete specimen. The strain measured here were, however, only reliable on the ascending part of the stress-strain curve.

Two test series were conducted at the Department establishing stress-strain curves of 4 different concretes. Two high strength concretes with a compressive strength on the 90 MPa level and 70 MPa level, and two normal strength concretes on the 50 MPa level and 40 MPa level.

All successfully established stress-strain curves can be seen in Olsen [2], but some examples of stress-strain curves are shown in Fig. 2.4.

### 2.3 Mathematical Representation of the Stress-Strain Curves.

The obtained stress-strain curves for each of the above mentioned four types of concrete, were represented mathematically by the following analytic expression:

$$y = \begin{cases} \frac{A_a \cdot x + B_a \cdot x^2}{1 + C_a \cdot x + D_a \cdot x^2} , & 0 \leq x \leq 1 \text{ (Ascending part)} \\ \frac{A_d \cdot x + B_d \cdot x^2}{1 + C_d \cdot x + D_d \cdot x^2} , & x > 1 \text{ (Descending part)} \end{cases}$$

where

$$y = \sigma_c / \sigma_{co} \quad , \quad x = \epsilon_c / \epsilon_{co}$$

$\sigma_c$  and  $\epsilon_c$  are stress and strain in general.

$\sigma_{co}$  and  $\epsilon_{co}$  are peak stress and corresponding strain.

$A_a$ ,  $B_a$ ,  $C_a$  and  $D_a$  constants for the ascending part of the stress-strain curve.

$A_d$ ,  $B_d$ ,  $C_d$  and  $D_d$  constants for the descending part of the stress-strain curve.

The constants in the mathematical expression can be generated from the knowledge of 3 key points on the experimental curves, namely:

- 1) Stress and strain at peak stress.
- 2) Secant modulus of elasticity on the ascending part at  $0.45 \times \sigma_{co}$ .
- 3) Stress and strain at the inflection point of the descending part.

A more detailed description of how constants are generated can be found in Olsen [2]. Table 2.1 give the average values of the three key points and the constants in the mathematical expression for each of the four concretes tested. In Fig. 2.5 is shown an example of a mathematical representation of a stress-strain curve compared to the experimental results from the testing of normal strength concrete on a 40 MPa level.

The above described mathematical expression has the following shortcomings, when the practical work in determine a stress-strain curve is considered:

- 1) Generating the constants for the mathematical expression is rather complexe since four equations need to be solved for the ascending as well as for the descending part of the stress-strain curve.
- 2) Knowledge of the complete experimentally obtained stress-strain curve is needed in order to establish the mathematical expression. This knowledge is, however, difficult to establish experimentally.

In the following a new and more practical mathematical expression is therefore suggested. This expression is very similar to the CEB proposal [7] and is based on information obtained through the previous expression. The suggested expression needs only knowledge of the ascending part of a stress-strain curve in order to gen

erate the complete stress-strain curve.

$$y = \begin{cases} \frac{\alpha \cdot x - x^2}{1 + (\alpha - 2) \cdot x} & 0 < x \leq 1 \quad (\text{Ascending part}) \\ \frac{k \cdot \alpha \cdot x - x^2}{1 + (k \cdot \alpha - 2) \cdot x + x^2} & x \geq 1 \quad (\text{Descending part}) \end{cases} \quad (2.2)$$

where

$$y = \sigma_c / \sigma_{CO}$$

$$x = \epsilon_c / \epsilon_{CO}$$

$$\alpha = E_c / E_{CO}$$

$$k = 485 \cdot \alpha / \sigma_{CO}^2 \quad \sigma_{CO} \text{ in MPa.}$$

$\sigma_c$  and  $\epsilon_c$  : Stress and strain in general.

$\sigma_{CO}$  and  $\epsilon_{CO}$  : Peak stress and corresponding strain.

$E_c$  : Secant modulus from the origin to a stress level of  $0.45 \times \sigma_{CO}$ .

$E_{CO}$  : Secant modulus from the origin to the peak compressive stress  $\sigma_{CO}$ .

From the experimentally obtained stress-strain curves formulas were established predicting the value of  $k$ ,  $\epsilon_{CO}$  and  $E_c$  by using least squares fitting procedures. The formula to predict  $\epsilon_{CO}$  and  $E_c$  is as follows

$$\epsilon_{CO} = 3.805 \cdot 10^{-3} - 7.261 \cdot 10^{-5} \cdot \sigma_{CO} + 5.975 \cdot 10^{-7} \cdot \sigma_{CO}^2$$

$$E_c = 6627 + 919 \cdot \sigma_{CO} - 4.857 \cdot \sigma_{CO}^2$$

It is now possible to generate the complete stress-strain curve of concrete produced with Danish materials, with the knowledge of only the compressive strength in the range of 40 MPa to 90 MPa. It must be emphasized however that since the suggested expression is based on experimentally obtained stress-strain curves, the generated curves will be influenced by the special measuring technic

and specimen characteristics used in the experiments. Some of these influences are described in Olsen [2].

From table 2.1 it can be seen, that the average compressive strength for the high strength concrete on the 90 MPa level was 91.9 MPa, while the average strength for the normal strength concrete on the 40 MPa level was 40.2 MPa. Using these average strength values a complete stress-strain curve is generated by the suggested more practical expression and compared to the first mentioned proposal.

From Fig. 2.6 and 2.7 it can be seen that the two expressions give very similar stress-strain curves and when comparing the two curves to the obtained curves, it can be seen that both give an equally good representation, and that differences in the two expressions can be considered negligible.

The more practical mathematical expression, which represent the uniaxial stress-strain curves of concrete, are used in the nonlinear model, see chapter 3.

### 3. NONLINEAR MODEL FOR CROSS-SECTIONAL ANALYSIS

#### 3.1 Introduction

Using nonlinear computerized analysis techniques makes it possible to predict the ultimate behavior of structural members when having knowledge of the concrete and steel stress-strain curves, cross-sectional properties and load conditions.

This investigation only looks into the ultimate strength of reinforced concrete rectangular members subjected to flexure and axial loads, and predicts the sectional ductility and rotational capacity of structural members subjected to pure bending.

The following sections describe the assumptions made in the nonlinear model and the technique used to calculate the ultimate strength of the structural members.

#### 3.2 Assumptions in the Nonlinear Model.

The following assumptions are made in the nonlinear model:

- a) The single basic assumption, that is always adopted (and certainly always in practical design), is, that sections that are plane before bending remain so after bending. In other words, the strain is linearly distributed across the depth of the section.
- b) It is assumed, that no slip occurs between the reinforcement and the surrounding concrete. The strain in the reinforcement can therefore be calculated, once the linear strain distribution across the section is known.

c) It is assumed, that the tensile strength of concrete is zero when performing calculations to determine the strength of a given section.

In order to analyse a section, it is necessary to make some assumptions regarding the relationship between stress and strain in the materials.

#### Stress-strain relationship of steel.

This investigation analyses not only sections with reinforcement in the tension zone but also double reinforced sections i.e sections reinforced both at the tension and the compression zones).

Since the aim of this investigation is to analyse the influence on ultimate strength made by increasing concrete compressive strength, a simple bilinear stress-strain relationship for the reinforcement is assumed.

The bilinear stress-strain relationship of reinforcement is shown in Fig. 3.1. In this nonlinear model the strength of steel in compression is assumed equal to that of steel in tension. The modulus of elasticity for steel is considered to be  $2.0 \cdot 10^5$  MPa.

#### Stress-strain response of concrete.

It is assumed, that the mathematical expression (2.2), given in section 2.3, can be used to describe the compressive stress distribution across the concrete section, once knowledge of the strains in the compression zone and the concrete compressive strength is established.

Use of stress-strain curves obtained in uniaxial compression to model the flexural response of concrete i.e. flexural curve has been investigated and periodically challenged and is still a con-



roversical topic, mainly because the exact nature of the strain gradient effect is yet to be fully understood.

Comparative studies of axial and flexural curves have been reported by various authors [8], [9], [10], [11] and [12]. Sturman, et al. [12], for example, concluded that the peak of the flexural curve was located at a strain 50 % higher and a stress about 20 % larger than the peak of the axial curve. Clark, et al. [8], on the other hand, found practically no difference between the curves up to maximum stress; beyond this point they concluded that the presence of a strain gradient increases the toughness of the stress-strain response in the case of flexural curves when compared to axial curves.

In spite of the above diverging viewpoints it is now generally accepted, primarily based on the subsequent work by Gosh and Handa [9], and Karsan and Jirsa [11], that:

- 1) Both the flexural - and the axial curves are essentially the same up to maximum stress.
- 2) Differences in the descending branch consists mainly of an upward shift of the curve when under a strain gradient.

Results of the studies outlined above were derived from tests on concrete mostly in the 20 MPa to 40 MPa compressive strength range. Recently Pastor et al. [13] has conducted experimental comparative studies of axial and flexural curves, not only in the range of normal strength concrete but also in the range of high strength concrete.

Pastor et al. [13], concluded, that it appears that differences do exist between flexural and axial curves as far as their descending branch is concerned. For a given concrete compressive strength, (at least up to a concrete compressive strength of 85 MPa), the post-peak slope of the flexural curve has a slightly tougher stress-strain response than corresponding axial curves regardless of the nature of the strain gradient. Furthermore Pastor [13]

concluded that as the strength of concrete increases, differences between the flexural and axial stress-strain response decreases.

From a practical standpoint the above mentioned considerations suggest, that the improvement in the properties of the compressive stress block due to the presence of a strain gradient will be lower for high strength concrete than for normal strength concrete. Consequently, the use of axial curves to predict the ultimate strength of flexural members will yield results, that become less conservative as the strength of the concrete increases. In turn, the use of axial curves to predict the true ultimate strength of flexural members should according to the above considerations yield increasingly accurate results as the compressive strength of the concrete increases.

The considerations outlined above must, however, be taken with some caution due to a hypothesis stated by Hillerborg [14]. In this Hillerborg has stated that the descending branch of the flexural curves in the concrete compressive zone of structural members subjected to flexure is strongly dependent of the depth of the compression zone. This suggests that using uniaxial stress-strain curves to predict the ultimate strength of flexural members may lead to false conclusions.

It is, however, apparent from Hillerborg [14] that further experimental work is needed to substantiate or modify this hypothesis.

### 3.3 Technique of the Analysis.

The technique of calculating the ultimate strength of rectangular beams subjected to pure bending is outlined in the following procedure.

Considering Fig. 3.2 an initial small value of concrete compressive strain,  $\epsilon_c$ , in the extreme fiber is considered. For this value of strain, the correct depth,  $h_c$ , of the neutral axis, is obtained by iteration, so as to satisfy equilibrium of the sec-

tion. To conduct the iteration establishing the correct depth of  $h_c$ , for a given value of  $\epsilon_c$ , the following formulas are needed.

$$\epsilon_{sc} = \epsilon_c \cdot \frac{(h_c - c_1)}{h_c}$$

$$\epsilon_{st} = \epsilon_c \cdot \frac{(h_{ef} - h_c)}{h_c}$$

Stresses in the compression steel and the tension steel is determined by the knowledge of the stress-strain relationship (see section 2.2).

Force equilibrium must be obtained, giving the formula

$$A_{st} \cdot \sigma_{st} = A_{sc} \cdot \sigma_{sc} + b \cdot \sigma_{co} \cdot h_c \cdot \frac{\epsilon_{co}}{\epsilon_c} \cdot \int_0^{x_c} y(x) dx$$

$$F_{st} = F_c + F_{sc}$$

where:

- $\sigma_{st}$  : Stress in tension reinforcement.
- $\sigma_{sc}$  : Stress in compression reinforcement.
- $\sigma_{co}$  and  $\epsilon_{co}$  : Peak stress and corresponding strain of the concrete stress-strain curve.
- $x_c$  :  $\epsilon_c / \epsilon_{co}$
- $Y(x)$  : Mathematical expression (2.2), representing the concrete stress-strain relationship.
- $F_{st}$  : Force in the tension reinforcement.
- $F_{sc}$  : Force in the compression reinforcement.
- $F_c$  : Force in the concrete.

When the equilibrium is obtained the correct location of the neutral axis is established and the bending moment  $M$  can be calculated from the formula

$$M = F_c \cdot \left[ h_{ef} - h_c + h_c \cdot \frac{\epsilon_{co}}{\epsilon_c} \cdot \frac{\int_0^{x_c} x \cdot y(x) dx}{\int_0^{x_c} y(x) dx} \right] + F_{sc} \cdot (h_t - c_1)$$

Once the correct location of the neutral axis,  $h_c$ , is found for a given value of  $\epsilon_c$ , one point in the non-dimensional moment-curvature curve ( $\mu$ - $\kappa$  curve) is obtained, where:

$$\mu = \frac{M}{b \cdot h_{ef}^2 \cdot \sigma_{co}}$$

$$\kappa = \frac{\epsilon_c}{h_c}$$

By repeating the procedure outlined above for increasing values of compressive strain in the extreme fiber, the entire non-dimensional moment-curvature curve for the section is established. The maximum moment is the ultimate strength.

Fig. 3.3 shows an example of a moment-curvature curve, using the procedure described above. In this case the concrete of the rectangular cross-section has a compressive strength of 90 MPa. The section is single reinforced with 90 % of balanced steel ratio. Balanced reinforcement is defined as the amount of steel which produces simultaneous crushing of concrete in compression and yielding of steel in tension.

The technique of calculating the ultimate strength of rectangular beams subjected to combined bending and axial loads follow nearly the same procedure as outlined above.

Considering Fig. 3.4, for a given value of eccentricity,  $e$ , of the axial load, an initial small value of concrete compressive strain,  $\epsilon_c$ , in the extreme fiber is assumed. For this value of strain, the correct depth,  $h_c$ , of the neutral axis is obtained by iteration. To conduct the iteration the following formula are needed:

$$\epsilon_{sc} = \epsilon_c \cdot \frac{(h_c - c_1)}{h_c}$$

$$\epsilon_{st} = \epsilon_c \cdot \frac{(h_{ef} - h_c)}{h_c}$$

From knowledge of the reinforcement stress-strain relationship the axial load can be calculated from the formula,

$$N = A_{sc} \cdot \sigma_{sc} + b \cdot \sigma_{co} \cdot h_c \cdot \frac{\epsilon_{co}}{\epsilon_c} \cdot \int_0^{x_c} Y(x) dx - A_{st} \cdot \sigma_{st} \quad (3.4)$$

$$N = F_{sc} + F_c - F_{st}$$

If, however, the value of  $h_c > h$

$$F_c = b \cdot \sigma_{co} \cdot h_c \cdot \frac{\epsilon_{co}}{\epsilon_c} \cdot \int_{x_n}^{x_c} Y(x) dx$$

where

$$x_n = \frac{(h_c - h) \cdot \epsilon_c}{h_c \cdot \epsilon_{co}}$$

The moment equilibrium must be obtained, giving the formula:

$$N \cdot e = F_{sc} \cdot (h/2 - c_1) + F_c \cdot \left[ h/2 - h_c + h_c \cdot \frac{\epsilon_{co}}{\epsilon_c} \cdot \frac{\int_0^{x_c} x \cdot Y(x) dx}{\int_0^{x_c} Y(x) dx} \right] - F_{st} \cdot (h_{ef} - h/2)$$

If  $h_c > h$

$$N \cdot e = F_{sc} \cdot (h/2 - c_1) + F_c \cdot \left[ h/2 - h_c + h_c \cdot \frac{\epsilon_{co}}{\epsilon_c} \cdot \frac{\int_{x_n}^{x_c} x \cdot Y(x) dx}{\int_{x_n}^{x_c} Y(x) dx} \right] - F_{st} \cdot (h_{ef} - h/2)$$

If equilibrium is obtained the correct location of the neutral axis is established for a given value of  $\epsilon_c$ . In turn one point of the moment-curvature curve ( $\mu-\kappa$  curve) is established and by repeating the procedure for increasing values of  $\epsilon_c$  the entire moment-curvature curve can be determined. The maximum moment and corresponding axial load,  $N$ , is one point on the non-dimensional  $\mu-\nu$  curve representing the ultimate strength of the section subjected to combined bending and axial load, where

$$\nu = \frac{N}{h \cdot h_{ef} \cdot \sigma_{co}}$$

The entire non-dimensional  $\mu-\nu$  curve can be determined by repeating the outlined procedure for different values of the eccentricity  $e$ .

## 4. DESIGN PROPOSAL

### 4.1 Introduction.

In this chapter a design proposal is described, capable of predicting the ultimate strength of rectangular beams subjected to pure bending or combined bending and axial load.

As described in chapter 2, the complete concrete stress-strain curves of four compressive strength levels were experimentally established and a suitable mathematical expression were found, fitting the experimentally obtained curves.

The ultimate strength capacity of beams was calculated for a wide variety of design situations by using the nonlinear model described in chapter 3.

From these results the following design proposal based on the same principals as the Danish Code DS 411 [1], is suggested.

### 4.2 Ultimate Moment Capacity.

Five major assumptions are made in the design proposal, when predicting the ultimate moment capacity:

1. Plane sections before bending remain plane after bending (Bernoulli's Hypothesis), therefore the strain distribution along the section is linear.
2. The tensile strength of the concrete is assumed to be zero.
3. The stress-strain curve of the reinforcing steel is known, often simplified to a bilinear curve.
4. The stress-strain curve for concrete, defining the magnitude and position of the compressive resultant, is known. In DS 411 and the following design proposal a simplified rectangular distribution of the compressive stress is assumed.

5. The ultimate compressive strain in the concrete at the most highly stressed compression fiber is limited. In DS 411 this value is 0.0035, while in the following proposal this value varies, depending on the concrete compressive strength.

The concrete compressive stress distribution in the concrete is in the design proposal, suggested to be rectangular and its magnitude is determined by two parameters,  $\beta$  and  $\eta$ , where  $\beta$  is the ratio of stress in the rectangular distribution to the compressive strength and  $\eta$  is the ratio of the depth of the rectangular distribution to the actual one. Fig. 4.1 shows the shape of the stress distribution.

The value of  $\eta$  is suggested to 0.7 regardless of the compressive strength in the range of 40 - 90 MPa, while  $\beta$  varies from 1.0 to 0.85 depending on the concrete compressive strength. Table 4.1 shows the values of  $\eta$  and  $\beta$ . The ultimate compressive strain in the concrete  $\epsilon_{cu}$ , is suggested in the design proposal to depend on the concrete compressive strength. The value of  $\epsilon_{cu}$  decreases with an increase in the concrete compressive strength in the range of 40 - 90 MPa. Table 4.1 shows the values of  $\epsilon_{cu}$ .

A comparison of the design proposal, DS 411 and the nonlinear model when predicting the ultimate moment capacity is shown in chapter 5 for a variety of design situations.

#### 4.3 Ultimate Capacity of Combined Bending and Axial Load.

This design proposal predicts the ultimate capacity of single symmetrical rectangular concrete sections, subjected to bending and axial load applied to the sectional centroid. The proposal is based on the same principles as the Danish Code DS 411, when determining the criterion for values of moment and axial load causing failure, in other words the interaction diagrams. The proposal covers only the situations where compressive concrete stress exists at the top face of the section.



Considering Fig. 4.2 and assuming that the section is under-reinforced, the interaction diagram is suggested to be determined by 4 points (B-E). The points correspond to the following situations:

B: Pure Bending.

C: Balanced state (strain equal to the ultimate compressive strain in the concrete at the top face and strain equal to the strain in the reinforcement at yield condition on the opposite side).

D: Strain equal to the ultimate compressive strain in the concrete on one side and zero strain in the reinforcement on the opposite side.

E: Uniformly distributed compressive strain across the section.

When establishing the interaction diagram in the case of a balanced - or over-reinforced section, only points B, D and E need to be determined. This is illustrated in Fig. 4.3.

When calculating point C and D it is assumed, that the ultimate compressive strain in the concrete is depending on the compressive concrete strength and equal to the value used when calculating point B. Furthermore, it is assumed that the compressive stress distribution in the concrete is rectangular and its shape is determined by the same two parameters  $\beta$  and  $\eta$  which were established when calculating point B.

When calculating point E it is assumed, that the uniformly distributed compressive strain has a value of 0.0018, regardless of the compressive concrete stress, and that the uniformly distributed concrete stress is the concrete compressive strength. The value of the strain is based on knowledge of the uniaxial stress-strain curves established at the department and described in Olsen [2]. These curves showed, that the strain at peak stress for the four concrete strengths tested were 0.0018, taken as an average.

## 5. DS 411 AND THE DESIGN PROPOSAL COMPARED TO THE NONLINEAR MODEL

### 5.1 Introduction

The purpose of this chapter is to study how well the design proposal fits the nonlinear calculated results, and to study the consequences of using the Danish Code DS 411 when calculating ultimate capacities of high strength concrete sections.

In section 5.2 DS 411 and the proposal is compared to the nonlinear model when used on a rectangular cross section subjected to pure bending with only tensional reinforcement, while in section 5.3 the studied cross-section contains compressive reinforcement.

In section 5.4 the proposal and DS 411 is compared to the nonlinear model when used on a rectangular cross-section subjected to combined bending and axial load.

### 5.2 Ultimate Moment Capacity without Compressive Reinforcement.

The calculations when comparing DS 411 and the proposal to the nonlinear model are conducted on a single symmetrical rectangular cross-section. The width of the section is 0.5 m, the depth to the centroid of the tensional reinforcement is 0.9 m and the total height is 1.0 m. The stress-strain curve of the reinforcement is assumed to be bilinear and the ultimate moment is perpendicular to the symmetrical axis as shown in Fig. 4.1..

The comparison of DS 411 and the proposal to the nonlinear model is limited to cross-sections with a mechanical ratio of reinforcement,  $\omega$ , in the range of 0 to 1.0 and concrete compressive strength in the range of 40 - 90 MPa.

Figs. 5.1 to 5.6 shows, the  $\mu$ - $\omega$  curves of DS 411, the proposal and the nonlinear model for concrete of 6 different concrete compressive strengths. The following can be seen from the figures:

- When the cross-section is under-reinforced according to the nonlinear model i.e. yielding of the tensile reinforcement prior to ultimate capacity, the ultimate capacity can be estimated by DS 411 as well as by the proposal with results showing negligible deviations from the nonlinear model.
  
- The Danish code overestimates the balanced steel ratio, regardless of the compressive strength of the concrete. This is illustrated more clearly in Fig. 5.7, where the mechanical balanced reinforcement ratio is shown as a function of the concrete compressive strength. From this figure it can be seen, that the mechanical balanced reinforcement ratio, determined by the proposal is close to and on the conservative side of the results from the nonlinear calculations.
  
- When the cross-section is over-reinforced the Danish Code overestimates the ultimate capacity, while the proposal is closer to the results from the nonlinear model. The maximum deviations of the proposal and DS 411 compared to the nonlinear results are shown on table 5.1. From this table it can be seen that the maximum deviations of DS 411 are in the range of -11 % to -32 %, while the maximum deviation range of the proposal is of -1.8 % to +3.0 %. + indicates, that the deviation is on the conservative side.

From the above observations it can now be concluded, that the Danish Code DS 411 overestimates the balanced reinforcement ratio and the ultimate moment capacity of over-reinforced sections containing only tension reinforcement when using concrete with compressive strength in the range 40 - 90 MPa.

It must, however be emphasized, that the experimental results [8] - [13], indicates that using uniaxial stress-strain curves to predict the ultimate capacity of flexural members may lead to conservative results, especially in case of normal strength concrete, see section 3.2. As a result the overestimations by the Danish code may therefore be less in cases of normal strength concrete sections.

### 5.3 Ultimate Moment Capacity with Compression Reinforcement.

The calculations when comparing DS 411 and the proposal to the nonlinear model are conducted on the same cross-section as described in section 5.2. The depth to the centroid of the compressive reinforcement is 0.1 m and the stress-strain curve of the compressive steel is shown in Fig. 3.1.

The comparison is limited to cross-sections with a mechanical tension steel ratio in the range of 0 to 1.0. Furthermore, the ratio between compressive and tension reinforcement amount is limited to the values 0.2, 0.4 and 0.6.

Figs. 5.8 - 5.13 show the  $\mu$ - $\omega$  curves for DS 411, the proposal and the nonlinear model for 6 different concrete compressive strengths and the 3 compressive steel amounts.  $\omega$  indicate the tensional mechanical reinforcement ratio.

From these figures the following can be seen:

- As the ratio of compressive steel increases the balanced mechanical steel ratio of the tension reinforcement increases. This is illustrated in more detail in the figures 5.14 - 5.19. From these figures it can be seen, that the Danish code overestimates the balanced reinforcement ratio regardless of the concrete compressive strength and the compressive steel ratio. It can also be seen, that the balanced mechanical reinforcement ratio estimated by using the proposal becomes increasingly conservative as the compressive reinforcement increases.
- The  $\mu$ - $\omega$  curves, when using DS 411 and the proposal deviates from the  $\mu$ - $\omega$  curve of the nonlinear calculations. Table 5.2 shown the maximum deviations of DS 411 and the proposal, when the section is under-reinforced and over-reinforced compared to the nonlinear  $\mu$ - $\omega$  curve. From this table it can be seen, that DS 411 over-estimates the ultimate moment capacity as much as 8.3 % in the case of under-reinforced 70 MPa concrete sections, where the compressive steel ratio is 0.4 of

the tensile steel amount. While in cases of over-reinforced sections DS 411 over-estimates the ultimate moment as much as 37.3 % in cases of 70 MPa concrete and sections with compressive steel ratio of 0.2. Furthermore, it can be seen, that the  $\mu-\omega$  curve of the proposal is considerably closer to the nonlinear  $\mu-\omega$  curve regardless of the concrete compressive strength and in cases of compressive steel ratio of 0.2. As the compressive steel ratio increases the ultimate moment capacity estimated from the proposal becomes more conservative, up to as much as 17.4 % in cases of over-reinforced 90 MPa sections with a compressive steel ratio of 0.6.

From the above observations it can be concluded, that the Danish Code also in cases of sections with compressive reinforcement over-estimates both the balanced reinforcement ratio and ultimate moment capacity when using concrete with compressive strength in the range 40 - 90 MPa. The proposal, however, seems to be better but becomes conservative with increasing amount of compressive steel.

As mentioned in section 5.2 and 3.2 the  $\mu-\omega$  curves calculated from the nonlinear model may lead to somewhat conservative results especially in cases of normal strength concrete. In turn the over-estimation by the Danish code may be less than concluded above.

#### 5.4 Ultimate Capacity of Combined Bending and Axial Load.

The calculations when comparing DS 411 and the proposal with the nonlinear model are conducted on single symmetrical rectangular cross-sections. The geometry of the cross-sections is the same as described in section 5.3.

This comparison covers only the situation where compressive concrete stress exists at the top face of the section. Furthermore the comparison is limited to cover nine reinforcement degrees for each of the six concrete compressive strengths investigated.

The nine reinforcement degrees are divided into 3 compressive reinforcement amounts:

- No reinforcement in the compression zone of the section,  $\omega_c = 0$ , where  $\omega_c$  is the mechanical compressive steel ratio.
- Compressive steel amount is 50 % of the tensional steel amount,  $\omega_c = 0.5 \cdot \omega$ , where  $\omega$  is the mechanical tensional steel ratio.
- Equal amount of tension and compressive reinforcement,  $\omega_c = \omega$ .

For each of these compressive reinforcement degrees 3 tensional reinforcement amounts are used:

- $\omega = 0.5 \cdot \omega_{bal}$
- $\omega = \omega_{bal}$
- $\omega = 1.5 \cdot \omega_{bal}$

where  $\omega_{bal}$  is the balanced mechanical reinforcement ratio, estimated from the nonlinear model in the case of pure bending without compressive reinforcement.

Fig. 5.20-5.37 show the  $\mu$ - $\nu$  relationships for 6 different concrete strengths and 9 different reinforcement degrees. From these figures the following can be seen:

- The Danish Code, DS 411, over-estimates in general the ultimate capacity of sections subjected to combined bending and axial load, regardless of the concrete compressive strength and the reinforcement degree. The non-conservatism of DS 411 is, however, more pronounced in cases of high strength concrete.
- The proposal is in general considerably closer to the results from the nonlinear model, and is not solely conservative.

Table 5.3-5.8 gives the maximum deviations of the  $\mu-N$  curves estimated from the Danish and the proposal when compared to the nonlinear  $\mu-N$  curve. Not only the maximum conservative deviations are given but also the maximum non-conservative deviations.

From these tables it can be seen that the Danish code over-estimates the ultimate capacity of high strength concrete sections with -29 % taken as an average. While the average maximum deviations of the proposal in the case of high strength concrete sections are in the range of -3 % to +5 %, where - indicates the nonconservative cases.

In the case of normal strength concrete it can be seen from the tables 5.3-5.8, that the Danish code over-estimates the ultimate capacity with 14 % taken as an average, while the proposals average maximum deviations are in the range of -5 % to +5 %.

From the observations made above it can now be concluded, that the Danish Code, DS 411, seems to over-estimate the ultimate capacity of high strength concrete sections subjected to combined bending and axial load. The Danish Code is also in cases of normal strength concrete sections on the non-conservative side. It must, however, be emphasized, that using axial stress-strain curves to predict the ultimate capacity especially of normal strength concrete sections may lead to conservative results, and as a result the Danish Code may be less non-conservative (see section 5.2).

The suggested proposal seems to give a better estimate of the ultimate capacity of normal - and high strength concrete sections subjected to combined bending and axial load, but is not always on the conservative side.

## 6. DUCTILITY INDEX AND ULTIMATE PLASTIC ROTATION

### 6.1 Introduction

It is generally accepted that the stress-strain curve of high strength concrete in uniaxial compression reflects a more brittle behavior than for normal strength concrete. This was also observed on stress-strain curves from uniaxial compression tests of high and normal strength concretes produced with Danish materials [2].

The purpose of this chapter is therefore to illustrate the effect of increasing compressive concrete strength on the brittleness of reinforced high strength concrete structural elements. The illustration is based on calculated results originating from the previously described nonlinear model.

Brittleness of reinforced structural elements can be quantitatively expressed by ductility indices or the ultimate plastic rotation. Ductility and plastic rotation depend not only on the compressive stress-strain curve of concrete, but also on the amount of tensional longitudinal reinforcement, the amount of compressional longitudinal reinforcement, shape of the beam cross-section and presence of axial loads, as well as many other factors.

In the following section the terms ductility index and the ultimate plastic rotation used in this report will be defined, followed by an illustration of the effect of increasing concrete strength on these properties.

### 6.2 Definitions

The amount of post-peak deformation that unreinforced concrete can sustain before failure, is commonly referred to as the material ductility. If the amount is small or nil, the response is said to be brittle, if the post-peak deformation is significant, the response is said to be ductile.



In under-reinforced concrete beams, the term ductility is associated with the amount of deformation, that can be sustained after yielding of the tensile steel. It is quantitatively expressed as the ratio of the ultimate deformation divided by the deformation at first yield.

If the deformations are strural member deflections, the ratio is obtained from load-deflection relationships and expressed as:

$$\delta_d = \Delta_u / \Delta_y$$

$\delta_d$  = Displacement ductility index.

$\Delta_y$  = Deflection at first yield of the tensile steel.

$\Delta_u$  = Deflection at ultimate (failure) load.

Similarly, if deformations are sectional curvatures, the ratio is obtained from moment - curvature relationships and expressed as:

$$\delta_c = \kappa_u / \kappa_y$$

$\delta_c$  = Curvature ductility index.

$\kappa_y$  = Curvature at first yield of the tensile steel.

$\kappa_u$  = Curvature at ultimate (failure) load.

Both indices are related since deflection is a function of the second integral of the curvature along the member. It should be noted, however, that the curvature ductility index applies to a specific cross-section only, while the displacement ductility index on the other hand, applies to the beam as a structural unit. Consequently numerical values of  $\delta_d$  and  $\delta_c$  usually differ.

The curvature ductility index is in this report used to illustrate the effect of increasing compressive strength on the brittleness of structural members. The curvature at ultimate (failure) load is here defined as the curvature at which the moment on the post-peak moment-curvature relationship reaches a value of 95 % of the maximum moment. See Fig. 6.1.

As mentioned in section 6.1 ultimate plastic rotation is another term for quantitatively expressing the brittleness of reinforced

structural elements. Sufficient plastic rotation especially in continuous structural systems is of importance, since this makes it possible for redistribution of stresses to take place, thus leading to higher ultimate load for the total structure.

The ultimate plastic rotation in this report is expressed as

$$\theta_{pl} = (\kappa_u - \kappa_Y) \times L_{pl}$$

$\theta_{pl}$  = Ultimate plastic rotation in radians

$\kappa_Y$  = Curvature at first yield of the tensile steel

$\kappa_u$  = Curvature at ultimate (failure) load, defined above in this section.

$L_{pl}$  = The plasticity length of the plastic hinge.

In this report the plasticity length,  $L_{pl}$ , is assumed to be equal to the depth of the centroid of the tensional reinforcement,  $h_{ef}$ .

### 6.3 Ductility

The effect of increasing concrete compressive strength on the curvature ductility index,  $\delta_c$ , is illustrated below by calculated results from the previously described nonlinear model.

Fig. 6.2 show  $\delta_c$  as a function of  $\omega/\omega_{bal}$ , in the case of single symmetrical rectangular cross-sections with only tensional reinforcement and subjected to pure bending. The cross-sections geometry is equal to the one described in section 5.2. Furthermore Fig. 6.3 shows  $\delta_c/\delta_{c,40 \text{ MPa}}$  as a function of  $\omega/\omega_{bal}$ , where  $\delta_c/\delta_{c,40 \text{ MPa}}$  indicate the ratio between ductility indices, originating from sections with concrete compressive strengths in the range from 50 MPa to 90 MPa, and ductility index from sections with concrete compressive strength on a 40 MPa level.

From Fig. 6.2 and 6.3 it can be seen, that the ductility index decreases as the concrete compressive strength increases, regardless of the reinforcement ratio. It can also be seen that the relative ductility  $\delta_c/\delta_{c,40 \text{ MPa}}$  for high strength concrete, with

compressive strength in the range of 70 MPa-90 MPa, seems to be a lower bound of ductility for high strength concrete, with a minimum of only 0.78 in the case of  $\omega/\omega_{bal} \sim 0.6$ .

Fig. 6.4 show  $\delta_c$  as a function of the tensional mechanical reinforcement ratio. Two curves represent calculations conducted on sections subjected to pure bending and concrete with compressive strength of 40 MPa and 90 MPa, and tension reinforcement only. Fig. 6.4 also show curves representing calculations of sections with concrete on a 90 MPa level and with a compressive steel ratio 0.2, 0.4 and 0.6 of the tensional steel amount. The compressive steel is placed in the rectangular cross-section with the centroid at a depth of  $0.1 \times h_{ef}$ .

From Fig. 6.4 it can be seen that improvement of the ductility for sections of concrete on a 90 MPa level is possible by adding compressive reinforcement. The amount of compressive steel necessary to improve the ductility to that of sections with 40 MPa is, however, in the range of 40 % to 60 % of the tensional reinforcement. Furthermore it can be seen, that improving the ductility by adding compressive reinforcement is only effective for rather high tensional and compressional reinforcement ratios.

Some of the above described theoretical trends are also observed experimentally. Pastor et al [12] showed experimentally, that deflection ductility,  $\delta_d$ , decreases with increasing concrete compressive strength. The rectangular beams were single reinforced so that  $\omega/\omega_{bal} \sim 0.56$  where  $\omega_{bal}$  was estimated according to ACI [15]. The deflection ductility decreased from 3.54 to 1.75 for concrete with compressive strength of 26 MPa respectively 59 MPa. Furthermore Pastor et al showed experimentally that compression zone reinforcement increases the deflection ductility of rectangular beams with concrete on a 60 MPa level. The deflection ductility index was increased by a factor in the range of 1.4 - 3.1 by adding a compressive steel ratio of 0.5. The rather wide range is, according to Pastor et al, caused by different amount of transverse reinforcement in the experimental tests.

It can now be concluded, that single reinforced rectangular beams subjected to pure bending and made of high strength concrete in the range of 50 to 90 MPa will exhibit less ductility than beams of normal strength concrete, for the same  $\omega/\omega_{bal}$  ratio. It is however possible to improve the lesser ductile high strength concrete beams by adding compressive reinforcement. On the other hand ductility of a beam designed for a specific bending moment can be improved by using high strength concrete because the  $\omega/\omega_{bal}$  ratio decreases and consequently the  $\delta_c$  ratio increases ( see Fig. 6.2).

The above observations suggests that caution must be shown, when high strength concrete is utilized in continuous structural systems, since the structural elements may not have the sufficient plastic rotation capability as could normally be expected.

#### 6.4 Ultimate Rotation Capacity.

Considerable work has been laid down in the past three decades in order to increase the rotational capacity of hinging regions in reinforced concrete beams, [16] - [26]. Most of this work, particularly [22], [23], [26], centered on research to increase the degree of confinement of the critical sections to the limit, leading to large increase in the rotational capacity of the plastic hinges and hence to a considerable increase in ductility.

Several emperical expressions are available for estimating the ultimate plastic rotation  $\theta_{pl}$ . The various empirical expressions of [17], [24], [25] give plasticity length values which depend on the effective depth section and distance between the critical section and the point of contraflexure in a continuous structural system. Furthermore, the expressions give maximum concrete strain as a function of the confining transverse steel, width of beam section and the contraflexure distance.

The shortcoming of the above mentioned empirical expression is, that no investigation is carried out regarding the effect of increasing concrete compressive strength on the ultimate plastic rotation in the high strength concrete range.

This section only illustrates theoretically the effect of increasing concrete compressive strength on the ultimate plastic rotation.

Fig. 6.5 show  $\theta_{pl}$  as a function of  $w/w_{bal}$  relationships for six different concrete compressive strengths. The curves are obtained from calculated results, using the nonlinear model as described in chapter 3. The calculations are conducted on single symmetrical, single reinforced rectangular cross-sections. The width of the section is 0.5 m, the depth to the centroid of the tensional reinforcement is 0.91 m and the total height is 1.0 m.

From Fig. 6.5 it can be seen, that for the same ratio of  $w/w_{bal}$ , the ultimate plastic rotation decreases as the concrete compressive strength increases. It must however be emphasized that the conclusion is based on the assumption, that  $L_{pl}$  is equal to the effective depth section, regardless of the concrete compressive strength.

It is apparent, that more experimental research is needed to study which effect high strength concrete has on the ultimate rotation capacity in order to substantiate the above theoretically obtained conclusion.

A large test series [27] has, however, recently been conducted at the Department of Structural Engineering in order to study which effect high strength concrete has on the ultimate rotation capacity of beams, but the conclusions from this investigation are not completed at present time.

## 7. CONCLUSION

The following conclusions can be made from the investigation presented in this report:

- 1) A practical mathematical expression is suggested being capable of generating a complete compressive stress-strain relationship for concrete produced with Danish materials and with compressive strength in the range of 40 to 90 MPa.
- 2) The consequences of predicting the ultimate capacity of reinforced high strength concrete sections by extrapolating the Danish Code was investigated by comparing DS 411 to calculated results using a knowledge of the complete uniaxial stress-strain curve for concrete and applying nonlinear computerized methods. The code over-estimates the ultimate moment capacity with as much as 33 %, while the code in the case of sections subjected to combined bending and axial load over-estimated the ultimate capacity with as much as 39 %.

Also in the case of reinforced sections of normal strength concrete the code over-estimated the ultimate capacity but less pronounced. In the case of ultimate moment capacity the over-estimation by the code was up to 21 %, and the same in the case of combined bending and axial load.

It must be emphasized, however, that using uniaxial stress-strain curves to predict the ultimate capacity of flexural members may lead to conservative results, especially in cases of normal strength concrete and thereby the over-estimation by the Danish Code may be less.

- 3) A simple design proposal is suggested, based on the same principles as the Danish Code. The design proposal covers concrete compressive strength in the range of 40 to 90 MPa and has more acceptable deviations from the results predicted when using the complete uniaxial stress-strain curves than the Danish Code.

In the design proposal, the concrete compressive stress distribution is assumed rectangular when calculating the ultimate moment capacity, and its magnitude is determined by the two parameters  $\beta$  and  $\eta$ , where only  $\beta$  varies with the concrete compressive strength. Also the ultimate compressive strain,  $\epsilon_{cu}$ , at the most highly stressed compression fibre varies with the concrete compressive strength.

In the following table the values  $\eta$ ,  $\beta$  and  $\epsilon_{cu}$  are given as a function of the concrete compressive strength which is not to be mistaken as the characteristic concrete compressive strength.

$f_c$ (MPa)	40	50	60	70	80	90
$\eta$	0.7	0.7	0.7	0.7	0.7	0.7
$\beta$	1.0	0.85	0.85	0.85	0.85	0.85
$\epsilon_{cu}$ (‰)	3.0	3.0	2.4	2.4	2.4	2.4

In the design proposal an interaction diagram based on the same principals as the Danish Code is established, when calculating ultimate capacity of sections subjected to combined bending and axial load, i.e. certain strain distributions across the section are assumed.

The concrete compressive stress distribution and  $\epsilon_{cu}$ , when establishing the interaction diagram is determined by the above table except in the case of point E of the interaction diagram. In the design proposal the uniformly distributed compressive strain across the section in the case of point E is assumed having the value 0.0018 regardless of the concrete compressive strength. The corresponding concrete stress is suggested to be the concrete compressive strength.

- 4) The curvature ductility of single reinforced rectangular high strength concrete sections was investigated by using a knowledge of the complete stress-strain curves of concrete.

It is concluded, that the ductility of high strength concrete sections is less than that of normal strength concrete sections, regardless of the reinforcement degree  $\omega/\omega_{bal}$ . Furthermore it seems, that high strength concrete in the range of 70 to 90 MPa show a lower bond of ductility, which seems to have a value of only 78 % of 40 MPa normal strength concrete sections when  $\omega/\omega_{bal} \sim 0.6$ .

It is also shown, that the less ductility of 90 MPa high strength concrete section can be improved by adding compressive reinforcement, but the degree of reinforcement must be in the range of 40-60 % of the tensional reinforcement.

Also the ultimate plastic rotation is investigated. It seems that also the ultimate plastic rotation,  $\theta_{pl}$ , decreases for increasing concrete compressive strength.

- 5) The above conclusions suggests, that caution must be taken when high strength concrete is utilized in structural systems. Not only can the ultimate capacity of structural elements be over-estimated, if the present Danish Code is used but sufficient plastic rotation capability may not exist in continuous structural systems.



## 8. REFERENCES

- [1] DS 411, "Dansk Ingeniørforenings norm for Betonkonstruktioner", Teknisk Forlag, Normstyrelsens Publikationer, NP-169-N, 1984.
- [2] Olsen, N.H., "Uniaxial Stress-Strain Curves of High Strength Concrete", Report R 232, Department of Structural Engineering, Technical University of Denmark, Lyngby 1988.
- [3] Brock, G., "Concrete: Complete Stress-Strain Curves", Engineering (London), V.193, No. 5011, May 1962, p. 606.
- [4] Barnard, P.R., "Researches into the Complete Stress-Strain Curve for Concrete", Magazine of Concrete Research (London), V16, No. 49, Dec. 1984, pp. 203-210.
- [5] Turner, P.W., and Barnard, P.R., "Stiff Constant Strain Rate Testing Machine", The Engineer (London), V.214, No. 5557, July 1962, pp. 146-148.
- [6] Sangha, C.M., and Dhir, R.K., "Strength and Complete Stress-Strain Relationships for Concrete Tested in Uniaxial Compression Under Different Test Conditions", Materials and Structures/Research and Testing (Paris), V.5, No. 30, Nov.-Dec. 1972, pp. 361-370.
- [7] Revision of CEB Model Code 1978, 1. Draft, Chapter 2, January 1988.
- [8] Clark, L.E., Gerstle, K.H., and Tulin, L.G., "Effect of Strain Gradient on the Stress-Strain Curve of Mortar and Concrete", "Journal of the American Concrete Institute, Vol. 64, No. 9, September 1967, pp. 580-586.
- [9] Ghosh, S.K., and Handa, V.K., "Strain Gradient and the Stress-Strain Relationship of Concrete in Compression," Highway Research Record, No. 324, Washington, D.C., 1970, pp., 44-53.

- [10] Hognestad, E., Hanson, N.W., and McHenry, D., "Concrete Stress Distribution in Ultimate Strength Design, "Journal of the American Concrete Institute Proceedings Vol. 52, No. 4, December 1955, pp. 455-480. Also PLA Development Bulletin D6.
- [11] Karsan, I.D., and Jirsa, J.O., "Behavior of Concrete Under Varying Strain Gradients," Journal of the Structural Division, American Society of Civil Engineers, Vol. 96, No. ST8, August 1970, pp. 1675-1696.
- [12] Sturman, G.M., Shah, S.P., and Winter, G., "Effect of Flexural Strain Gradients on Microcracking and Stress-Strain Behavior of Concrete," Journal of the American Concrete Institute, Proc. Vol. 62, No. 7, July 1965, pp. 805-822.
- [13] Pastor, J.A., Nilson, A.H., and Slate, F.O., "Behavior of High Strength Concrete Beams," Report 84-3, Department of Structural Engineering, Cornell University, February, 1984.
- [14] Hillerborg, A., "Fracture Mechanics Concepts Applied to Moment Capacity and Rotational Capacity of Reinforced Concrete Beams", Paper Presented at the International Conference on Fracture of Concrete and Rock, Vienna July 4-6, 1988.
- [15] American Concrete Institute Committee 318, "Building Code Requirements for Reinforced Concrete ACI-318-83)," American Concrete Institute, Detroit, Michigan, 1983, 111 pp.
- [16] Baker, A.L.L., "The ultimate load applied to the design of reinforced and prestressed concrete frames, Concrete Publications, London, 1956, 91 pp.
- [17] Baker, A.L.L. and Amarakone, A.M.N., Inelastic hyperstatic frame analysis. Flexural mechanics of reinforced concrete, American Concrete Institute, SP-12, pp. 85-142.

- [18] Baker, A.L.I., Limit state design of reinforced concrete, Cement and Concrete Association, London, 1970, 345 pp.
- [19] Base, G.L.D. and Read, J.B., Effectiveness of helical binders in the compression zone of concrete beams. J. Am. Concr. Inst. Proc. Vol. 62, No. 7, July 1965, pp. 763-779.
- [20] Mattock, A.H., Rotational Capacity of Hinging Regions in Reinforced concrete Beams. Flexural mechanics of reinforced concrete, American Concrete Institute, SP-12, 1964, pp. 143-181.
- [21] Cohn, M.Z. and Ghosh, S.K., Ductility of reinforced sections in bending. Proc. int. symp. inelasticity and non-linearity in struct. concr., University of Waterloo Press, June 1972, pp. 111-146.
- [22] Nawy, E.G., Danesi, R.F. and Gnosko, J.J., Rectangular spiral binders effects on the plastic hinge rotation capacity in reinforced concrete beams. J. Am. Concr. Inst. Proc. Vol. 65 No. 12, Dec. 1968, pp. 1001-1010.
- [23] Nawy, E.G. and Salek, F., Moment-rotation relationships of non-bonded post-tensional I- and T-beams, J. Prestressed Concr. Inst., Vol. 13, No. 4, Aug. 1968, pp. 40-55.
- [24] Sawyer, H.A., Design of concrete frames for two failure states. Flexural mechanics of reinforced concrete, American Concrete Institute, SP-12, 1964, pp. 405-431.
- [25] Corley, W.G., Rotational capacity of reinforced concrete beams. J. Struct. Div., Am. Soc. Civ. Eng., Vol. 92, No. ST5, Oct. 1966, pp. 121-146. Discussion by Mattock, A.H., No. ST2, April 1967, pp. 519-522.

- [26] Nawy E.G., and Polyondy, J.G., Moment-rotation, deflection and cracking of spirally bound, pretensioned, prestressed concrete flanged beams, Bureau of Engineering Research, Rutgers University, Bulletin No. 51, Sept. 1976, 124 pp.
- [27] Grunert, H.S., Unpublished Research Report, Department of Structural Engineering, Technical University of Denmark, Lyngby, 1988.

**9. TABLES**

Compressive strength level	90	70	50	40
$\sigma_{co}$ (MPa)	91.9	64.8	51.9	40.2
$\epsilon_{co}$ (°/oo)	2.177	1.623	1.627	1.860
$\epsilon_{c45}$ (°/oo)	0.825	0.643	0.558	0.510
$\sigma_{ci}$ (MPa)	32.2	46.0	33.0	30.0
$\epsilon_{ci}$ (°/oo)	3.030	2.190	2.580	3.150
A <sub>a</sub>	1.05314	1.15113	1.30540	1.62818
B <sub>a</sub>	-0.87542	-0.68222	-0.44744	-0.12031
C <sub>a</sub>	-0.94686	-0.84887	-0.69460	-0.37182
D <sub>a</sub>	0.12458	0.31778	0.55256	0.87969
A <sub>d</sub>	0.05941	0.22131	0.37778	0.83619
B <sub>d</sub>	0	0	0	0
C <sub>d</sub>	-1.94059	-1.77869	-1.62222	-1.16381
D <sub>d</sub>	1	1	1	1

Table 2.1 Average values of the three key points and the constants in the mathematical expression,  $\epsilon_{c45}$  is strain at a stress level of 45 % of peak stress, while  $\sigma_{ci}$  and  $\epsilon_{ci}$  is concrete stress and strain at the inflection point.

$f_c$ (MPa)	40	50	60	70	80	90
$\eta$	0.70	0.70	0.70	0.70	0.70	0.70
$\beta$	1.00	0.85	0.85	0.85	0.85	0.85
$\epsilon_{cu}$ ( $^{\circ}/\infty$ )	3.0	3.0	2.4	2.4	2.4	2.4

Table 4.1 Values of  $\eta$ ,  $\beta$  and  $\epsilon_{cu}$  for concrete compressive strength, in the range from 40 MPa to 90 MPa.

Concrete Compressive Strength (MPa)	Max Deviation of the Proposal (%)	Max Deviation of the Danish Code (%)
40	-1.4	-11.4
50	+2.3	-20.5
60	+0.9	-29.0
70	-1.8	-32.5
80	-0.9	-32.3
90	+3.0	-20.5

Table 5.1 Maximum deviations of the proposal and DS 411 when compared to the nonlinear model assuming pure bending and only tensional reinforcing steel. + indicates the conservative side.

Concrete Compressive strength (MPa)	$\frac{A_{sc}}{A_{st}}$	Maximum deviation of DS 411 in %		Maximum deviation of the proposal in %	
		Under-Reinfor.	Over-Reinfor.	Under-Reinfor.	Over-Reinfor.
40	0.2	-2.53	-8.43	+2.53	+2.63
	0.4	-1.82	-5.21	+4.46	+4.46
	0.6	-1.78	-	+6.55	-
50	0.2	-5.80	-19.7	+2.94	+3.16
	0.4	-6.32	-14.8	+5.26	+5.43
	0.6	-4.70	-6.87	+6.04	+6.25
60	0.2	-1.90	-30.4	+1.82	+3.49
	0.4	-6.33	-22.5	+7.59	+11.7
	0.6	-4.76	-11.8	+14.3	+15.8
70	0.2	-7.69	-37.3	-1.92	-2.43
	0.4	-8.33	-26.5	+2.78	+8.62
	0.6	-5.17	-13.3	+12.1	+14.7
80	0.2	-5.52	-31.8	0	+1.24
	0.4	-7.93	-22.0	+5.3	+10.2
	0.6	-5.04	-14.0	+12.6	+14.7
90	0.2	-6.67	-26.8	+3.32	+6.67
	0.4	-4.94	-18.3	+8.64	+13.8
	0.6	-4.55	-10.3	+16.6	+17.4

Table 5.2 Maximum deviation of DS 411 and the proposal when compared to the nonlinear  $\mu$ - $w$  curve in cases of cross-sections subjected to pure bending and containing compressive reinforcement. + indicates the conservative side.

$\frac{\omega}{\omega_{bal}}$	$\frac{\omega_c}{\omega}$	Maximum deviation DS 411 (%)	Maximum deviation Proposal (%)
0.5	0	-12.5	+2.38 (-8.33)
	0.5	-10.0	+2.08 (-6.82)
	1.0	- 8.12	+3.70 (-8.00)
1.0	0	-11.1	-5.56
	0.5	-7.69	+3.95 (-7.37)
	1.0	-6.45	+4.85 (-5.00)
1.5	0	-10.3	-4.41
	0.5	- 8.51	+5.58 (-5.66)
	1.0	- 5.33	+7.92 (-2.74)

Table 5.3 Maximum deviations of  $\mu-\nu$  relationships estimated from the Danish Code, DS 411, and the proposal when compared to the nonlinear results in cases of cross-sections with concrete on a 40 MPa level. (+ indicates the conservative side).



$\frac{\omega}{\omega_{bal}}$	$\frac{\omega_c}{\omega}$	Maximum deviation DS 411 (%)	Maximum deviation Proposal (%)
0.5	0	-20.8	+6.89
	0.5	-23.1	+2.44
	1.0	-18.8	+1.67 (-5.00)
1.0	0	-20.8	+6.25
	0.5	-18.8	+3.03 (-2.56)
	1.0	-14.3	+4.76 (-4.00)
1.5	0	-19.2	+6.25
	0.5	-17.5	+4.88 (-4.44)
	1.0	-13.0	+5.45 (-1.67)

Table 5.4 Maximum deviations of  $\mu$ - $\nu$  relationships estimated from the Danish Code, DS 411, and the proposal when compared to the nonlinear results in cases of cross-sections with concrete on a 50 MPa level. (+ indicates the conservative side).

$\frac{\omega}{\omega_{bal}}$	$\frac{\omega_c}{\omega}$	Maximum deviation DS 411 (%)	Maximum deviation Proposal (%)
0.5	0	-26.2	+3.33
	0.5	-31.3	+3.33
	1.0	-33.3	-2.67
1.0	0	-30.2	+3.13
	0.5	-30.4	+1.82 (-1.35)
	1.0	-30.8	+8.33 (-4.59)
1.5	0	-27.7	+3.85
	0.5	-28.8	+5.71 (-3.70)
	1.0	-22.8	+12.8 (-1.05)

Table 5.5 Maximum deviations of  $\mu-\nu$  relationships estimated from the Danish Code, DS 411, and the proposal when compared to the nonlinear results in cases of cross-sections with concrete on a 60 MPa level. (+ indicates the conservative side).

$\frac{w}{w_{bal}}$	$\frac{w}{w_c}$	Maximum deviation DS 411 (%)	Maximum deviation Proposal (%)
0.5	0	-35.0	+2.08
	0.5	-38.6	-2.27
	1.0	-35.8	-5.26
1.0	0	-33.3	+2.50 (-2.44)
	0.5	-35.2	-2.63
	1.0	-30.0	+5.71 (-5.88)
1.5	0	-30.4	+2.22 (-4.35)
	0.5	-33.8	+1.47 (-5.71)
	1.0	-26.6	+8.88 (-5.88)

Table 5.6 Maximum deviations of  $\mu$ - $\nu$  relationships estimated from the Danish Code, DS 411, and the proposal when compared to the nonlinear results in cases of cross-sections with concrete on a 70 MPa level. (+ indicates the conservative side).

$\frac{\omega}{\omega_{bal}}$	$\frac{\omega_c}{\omega}$	Maximum deviation DS 411 (%)	Maximum deviation Proposal (%)
0.5	0	-28.6	+1.79
	0.5	-33.3	+1.15 (-2.78)
	1.0	-30.4	+1.67 (-3.13)
1.0	0	-29.5	+1.08 (-2.38)
	0.5	-32.1	+1.79 (-2.67)
	1.0	-27.0	+7.35 (-4.44)
1.5	0	-30.4	+2.25 (-2.17)
	0.5	-30.3	+4.17 (-3.66)
	1.0	-23.7	+11.6 (-1.90)

Table 5.7 Maximum deviations of  $\mu-\nu$  relationships estimated from the Danish Code, DS 411, and the proposal when compared to the nonlinear results in cases of cross-sections with concrete on a 80 MPa level. (+ indicates the conservative side).

$\frac{\omega}{\omega_{bal}}$	$\frac{\omega_c}{\omega}$	Maximum deviation DS 411 (%)	Maximum deviation Proposal (%)
0.5	0	-26.2	+2.27
	0.5	-22.6	+2.27
	1.0	-25.0	+5.17
1.0	0	-26.1	+2.17
	0.5	-26.7	+6.67
	1.0	-20.7	+11.4
1.5	0	-27.1	+1.14
	0.5	-22.2	+10.3
	1.0	-16.4	+18.6

Table 5.8 Maximum deviations of  $\mu-\nu$  relationships estimated from the Danish Code, DS 411, and the proposal when compared to the nonlinear results in cases of cross-sections with concrete on a 90 MPa level. (+ indicates the conservative side).

10. FIGURES

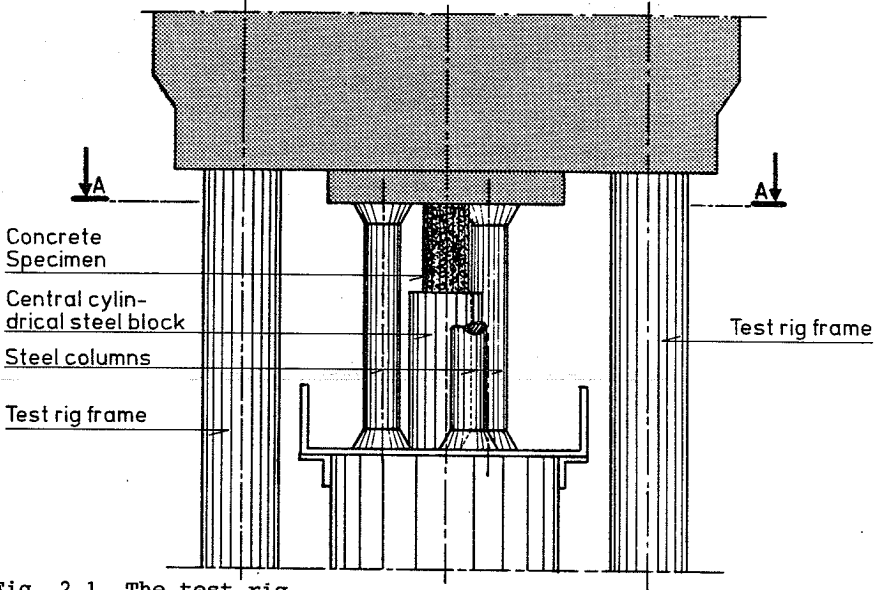


Fig. 2.1 The test rig.

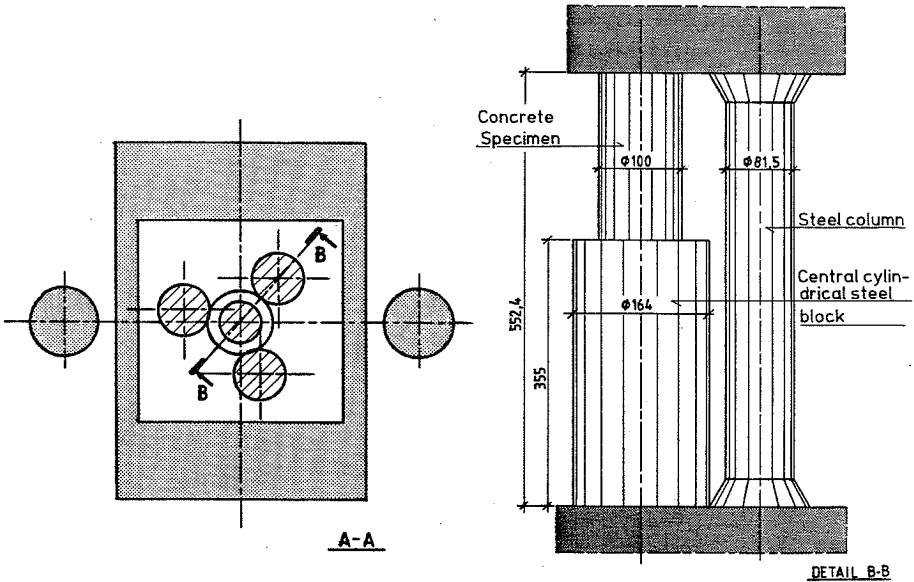


Fig. 2.2 Details of the test rig.

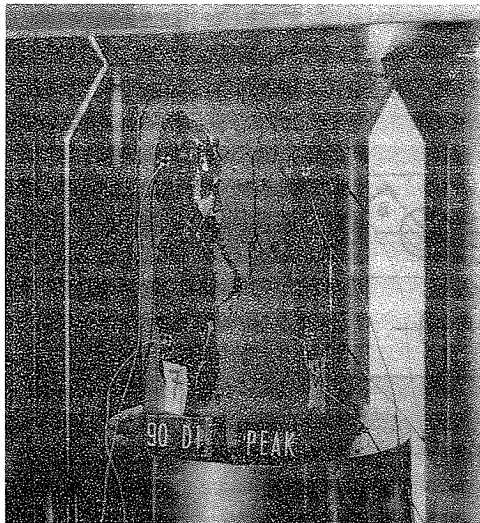
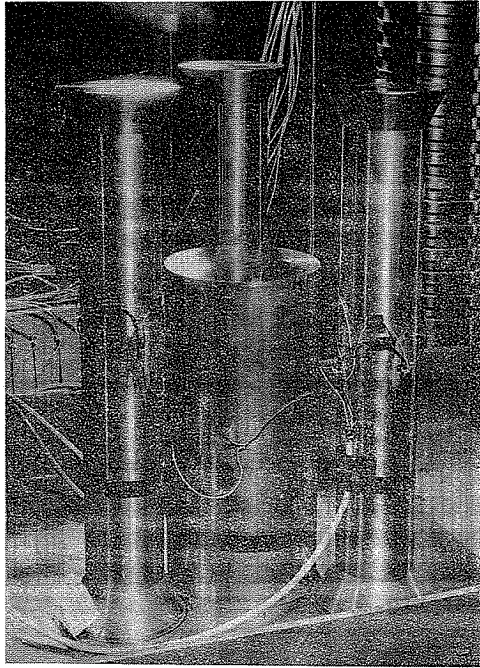


Fig. 2.3 Photo of the test rig.

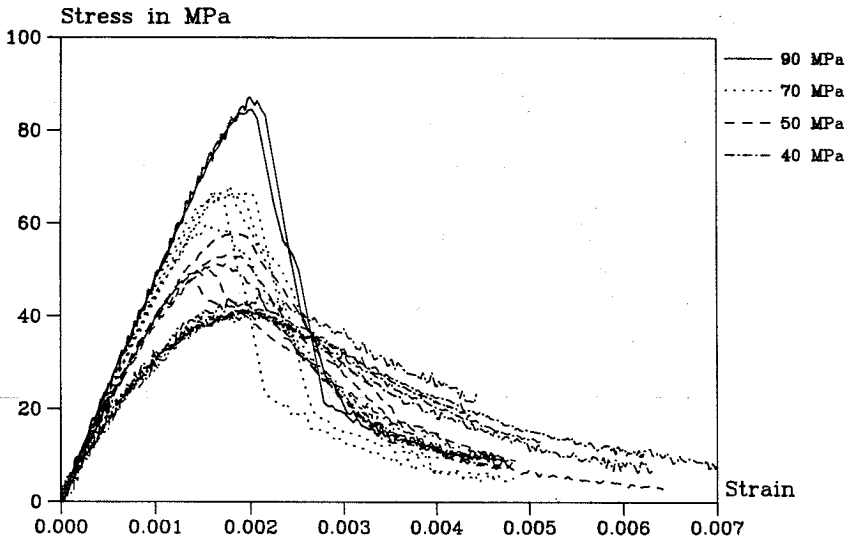


Fig. 2.4 Examples of obtained stress-strain curves.

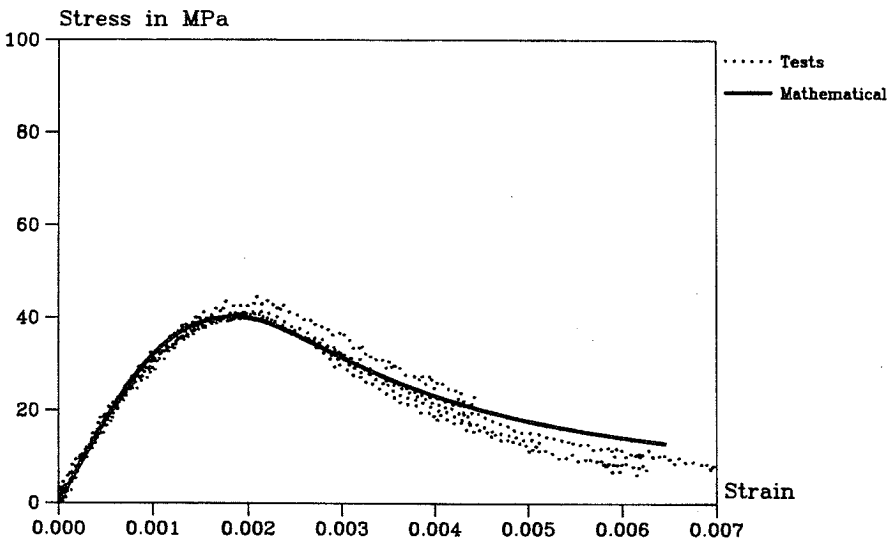


Fig. 2.5 An example of the mathematical fit to experimental results from normal strength concrete.



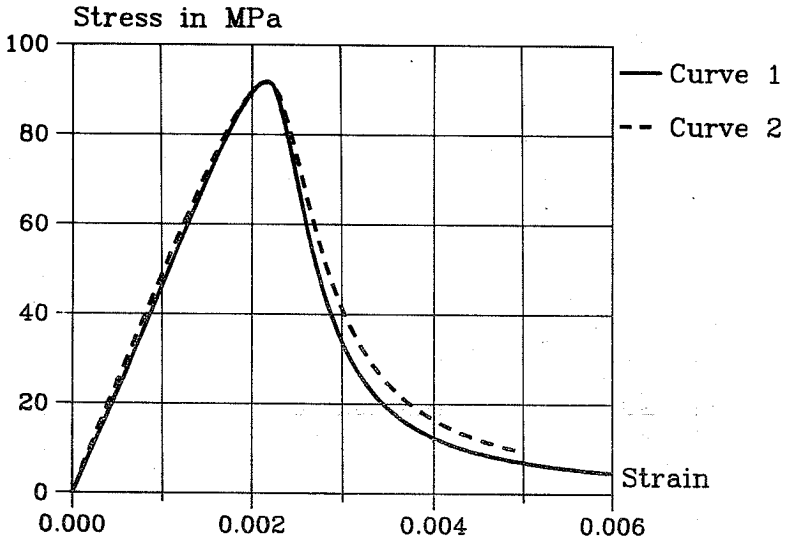


Fig. 2.6 Comparison between the first proposed expression and the suggested practical proposal in the case of high strength concrete on a 90 MPa level.

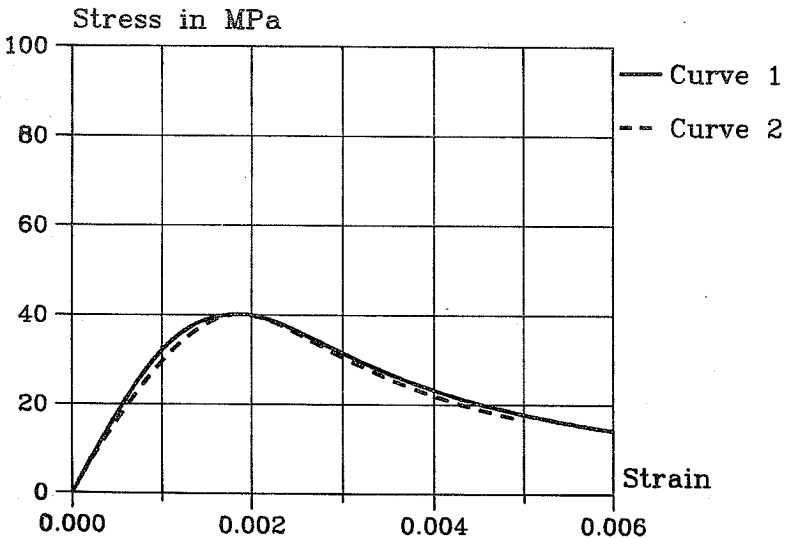


Fig. 2.7 Comparison between the first proposed expression and the suggested practical proposal in the case of normal strength concrete on a 40 MPa level.

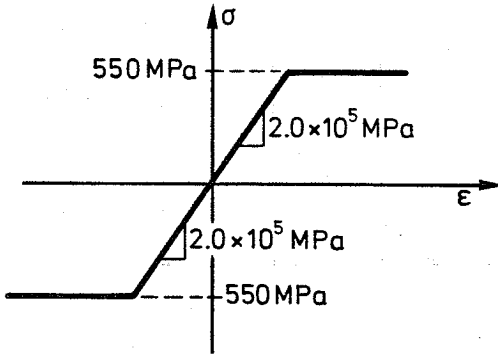


Fig. 3.1 Bilinear stress-strain relationship for the reinforcement steel used in the nonlinear analysis.

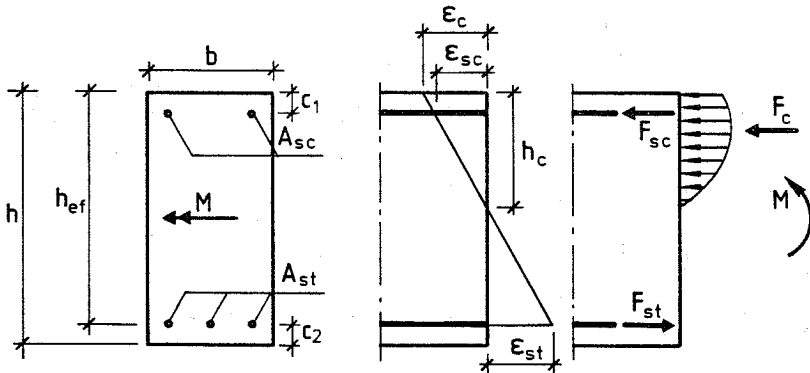


Fig. 3.2 Cross-section subjected to pure bending in the nonlinear model.

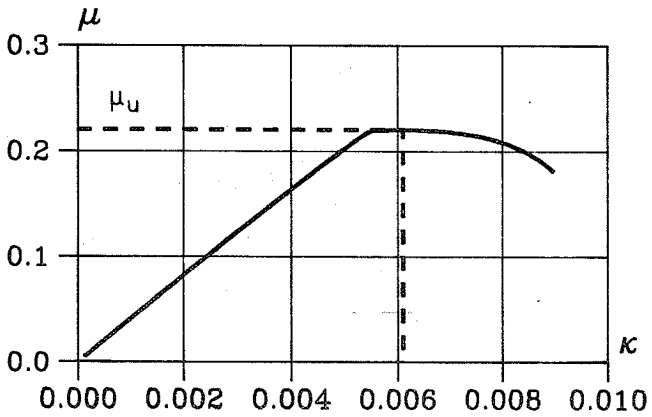


Fig. 3.3 An example of moment-curvature curve.

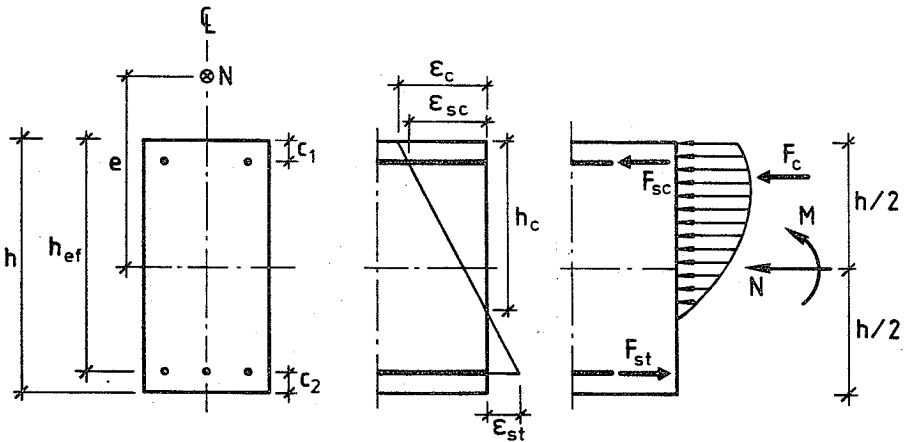


Fig. 3.4 Cross-section subjected to excentric axial load in the nonlinear model.

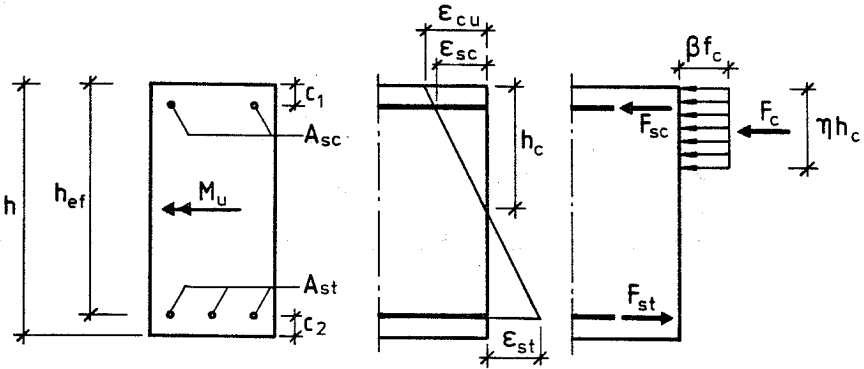


Fig. 4.1 Cross-section subjected to pure bending in the design proposal.

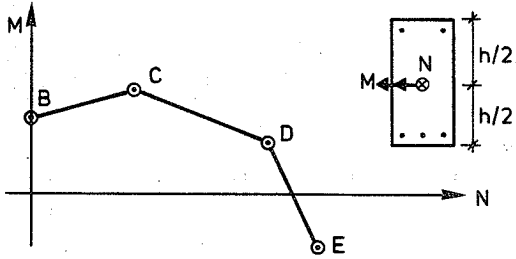


Fig. 4.2 Suggested interaction diagram when the section is under-reinforced.

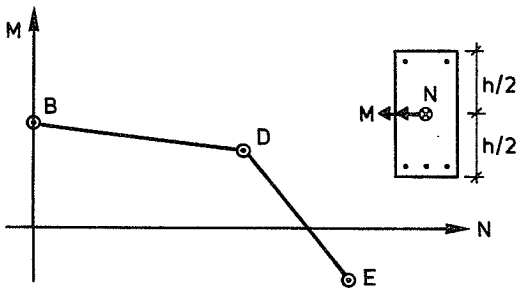


Fig. 4.3 Suggested interaction diagram when the section is balanced reinforced or over-reinforced.

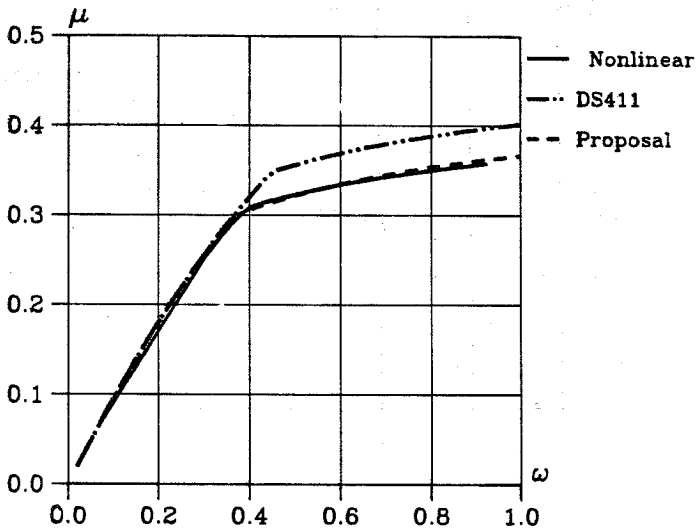


Fig. 5.1  $\mu$ - $\omega$  relationship of DS 411, the proposal and the nonlinear model in the case of pure bending, only tensional reinforcement and concrete compressive strength on a 40 MPa level.

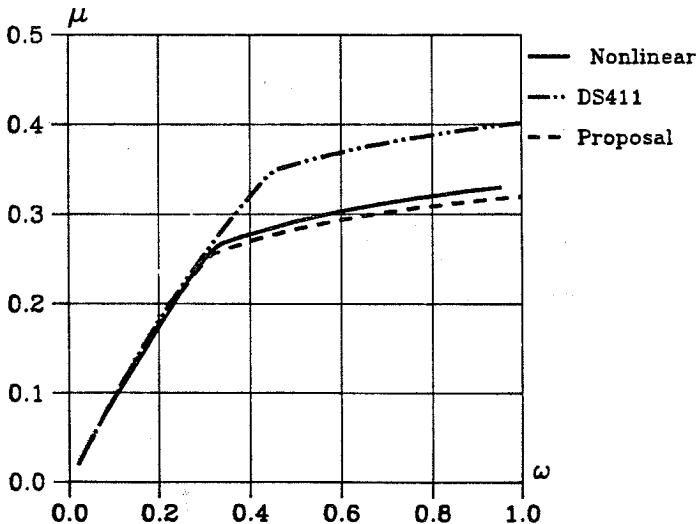


Fig. 5.2  $\mu$ - $\omega$  relationship of DS 411, the proposal and the nonlinear model in the case of pure bending, only tensional reinforcement and concrete compressive strength on a 50 MPa level.

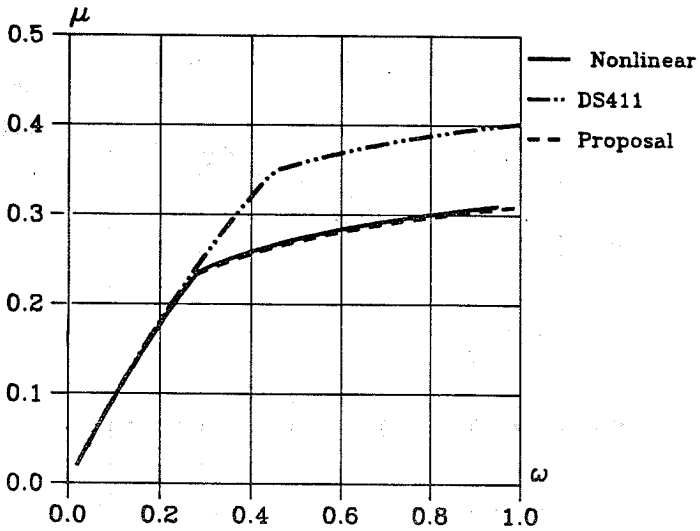


Fig. 5.3  $\mu$ - $\omega$  relationship of DS 411, the proposal and the nonlinear model in the case of pure bending, only tensional reinforcement and concrete compressive strength on a 60 MPa level.

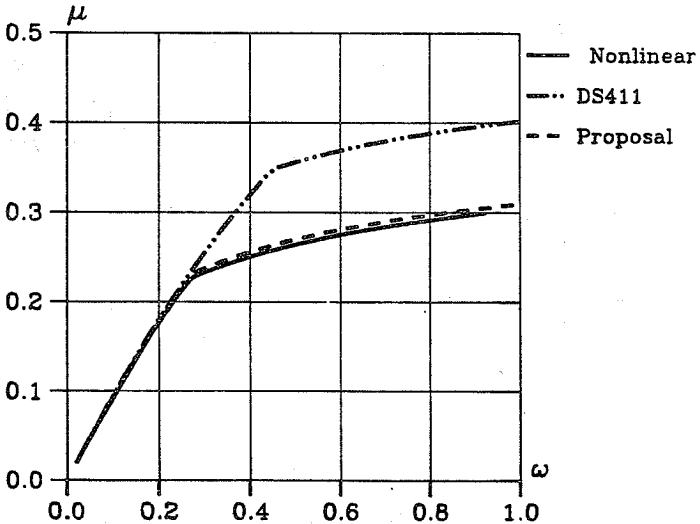


Fig. 5.4  $\mu$ - $\omega$  relationship of DS 411, the proposal and the nonlinear model in the case of pure bending, only tensional reinforcement and concrete compressive strength on a 70 MPa level.

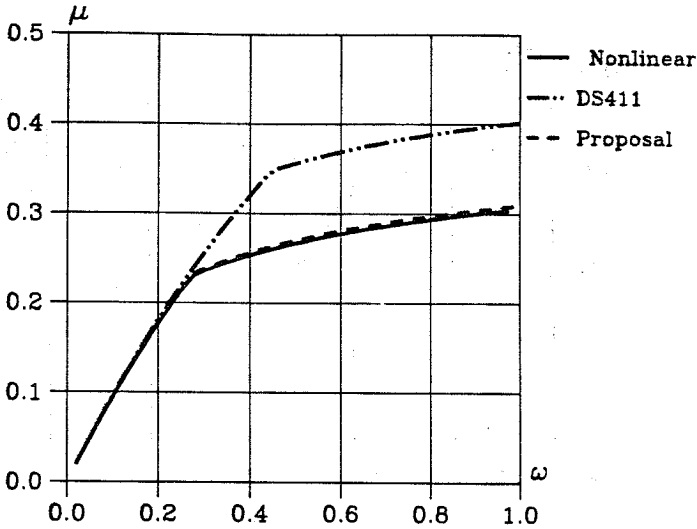


Fig. 5.5  $\mu$ - $\omega$  relationship of DS 411, the proposal and the nonlinear model in the case of pure bending, only tensional reinforcement and concrete compressive strength on a 80 MPa level.

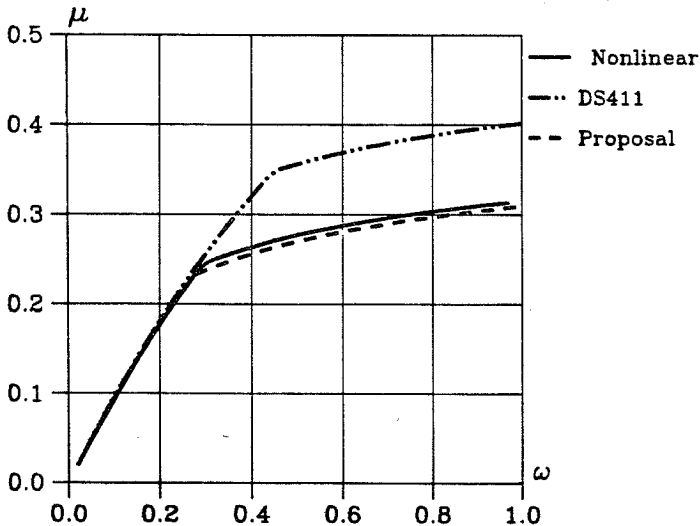


Fig. 5.6  $\mu$ - $\omega$  relationship of DS 411, the proposal and the nonlinear model in the case of pure bending only tensional reinforcement and concrete compressive strength on a 90 MPa level.



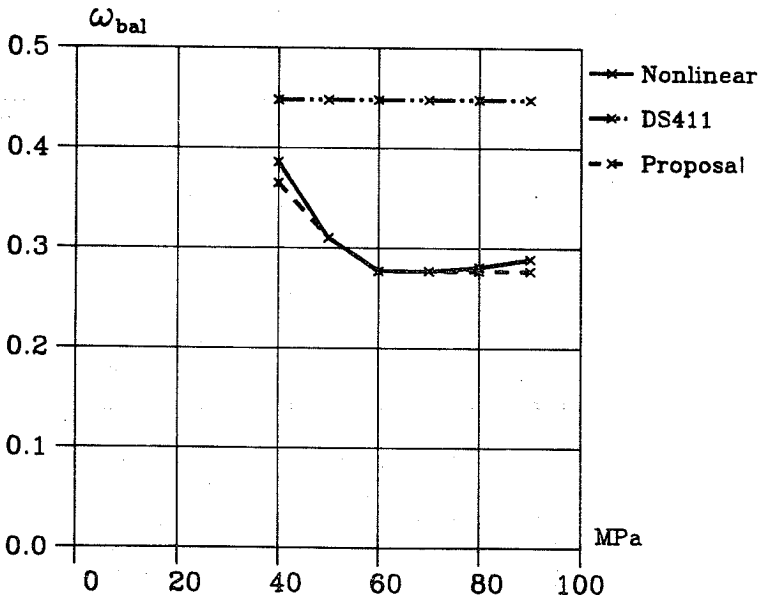


Fig. 5.7 Balanced mechanical reinforcement ratio as a function of the concrete compressive strength.

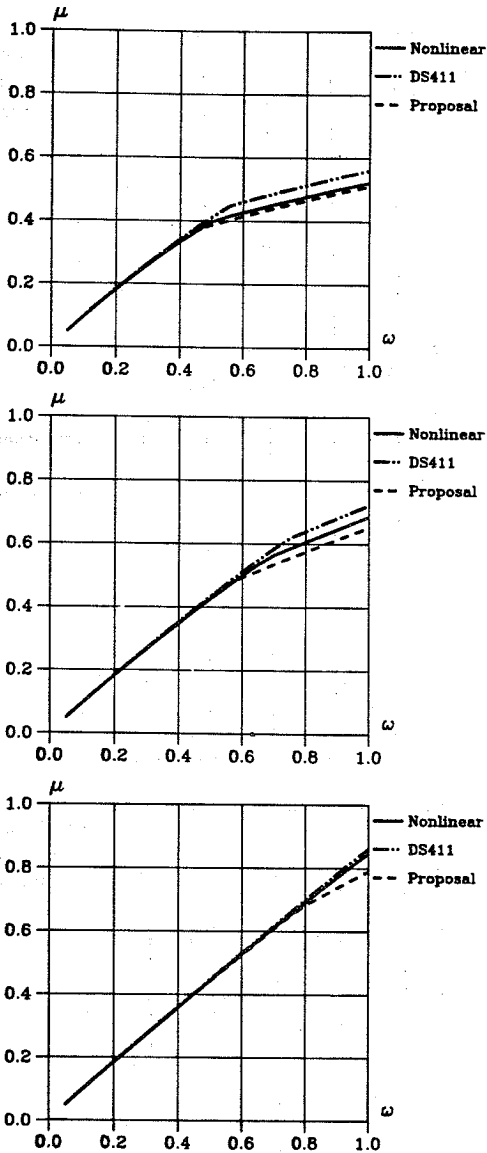


Fig. 5.8  $\mu$ - $\omega$  relationship of the Danish Code, DS 411, the proposal and the nonlinear model. The sections are subjected to pure bending and containing compressive steel ratios 0.2, 0.4 and 0.6 of the tensional steel amount. The concrete compressive strength of the section is on a 40 MPa level.

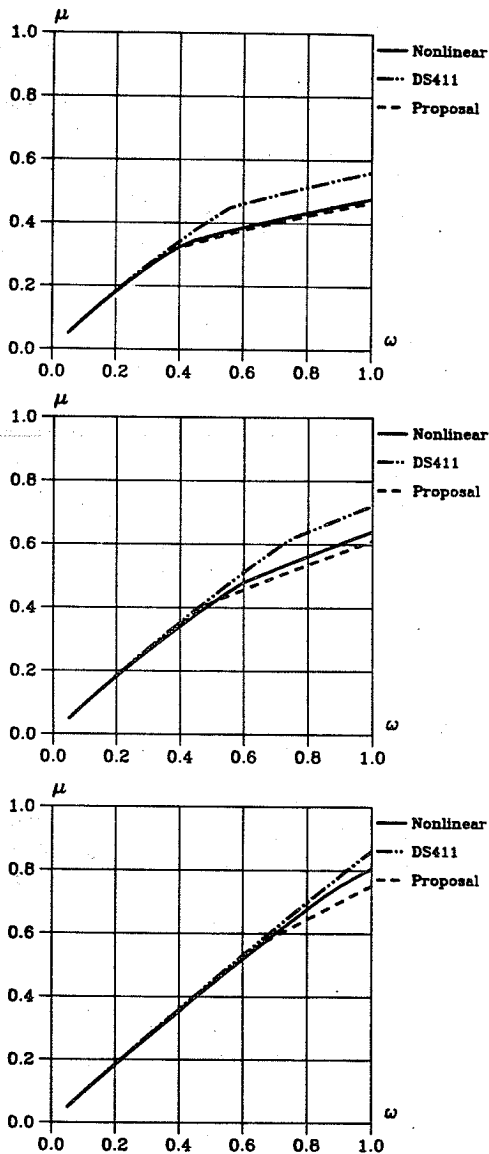


Fig. 5.9  $\mu$ - $\omega$  relationship of the Danish Code, DS 411, the proposal and the nonlinear model. The sections are subjected to pure bending and containing compressive steel ratios 0.2, 0.4 and 0.6 of the tensional steel amount. The concrete compressive strength of the section is on a 50 MPa level.

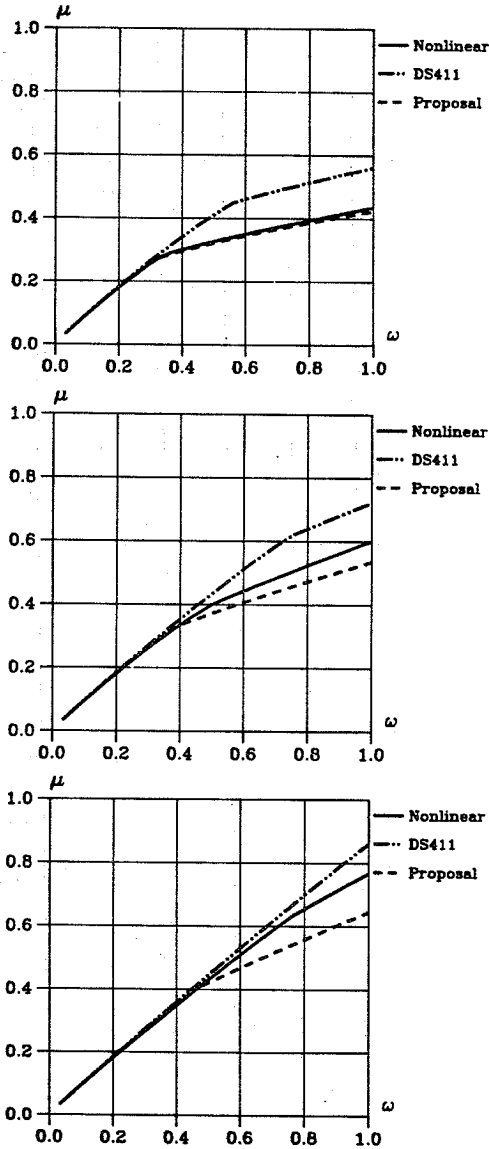


Fig. 5.10  $\mu$ - $\omega$  relationship of the Danish Code, DS 411, the proposal and the nonlinear model. The sections are subjected to pure bending and containing compressive steel ratios 0.2, 0.4 and 0.6 of the tensional steel amount. The concrete compressive strength of the section is on a 60 MPa level.

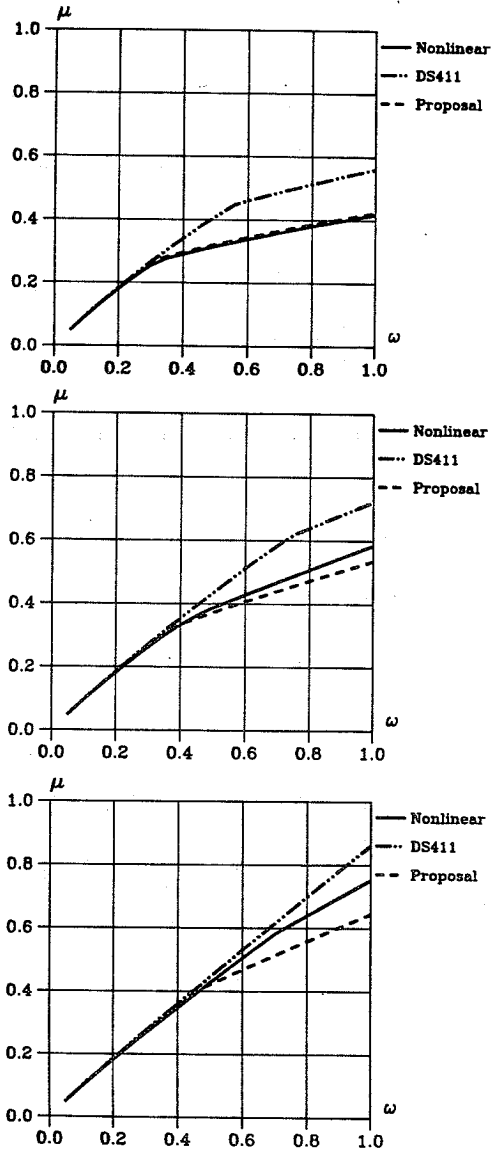


Fig. 5.11  $\mu$ - $\omega$  relationship of the Danish Code, DS 411, the proposal and the nonlinear model. The sections are subjected to pure bending and containing compressive steel ratios 0.2, 0.4 and 0.6 of the tensional steel amount. The concrete compressive strength of the section is on a 70 MPa level.

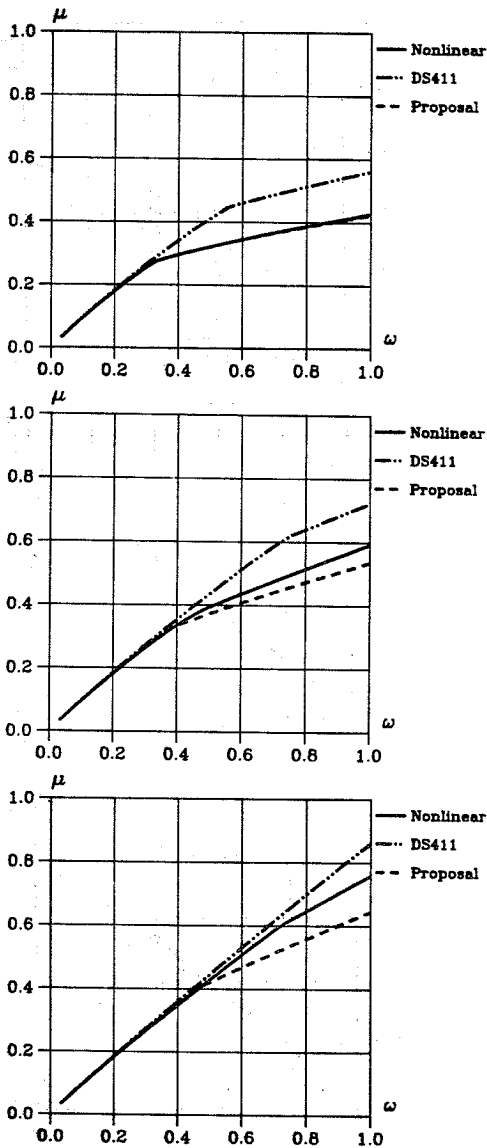


Fig. 5.12  $\mu$ - $\omega$  relationship of the Danish Code, DS 411, the proposal and the nonlinear model. The sections are subjected to pure bending and containing compressive steel ratios 0.2, 0.4 and 0.6 of the tensional steel amount. The concrete compressive strength of the section is on a 80 MPa level.

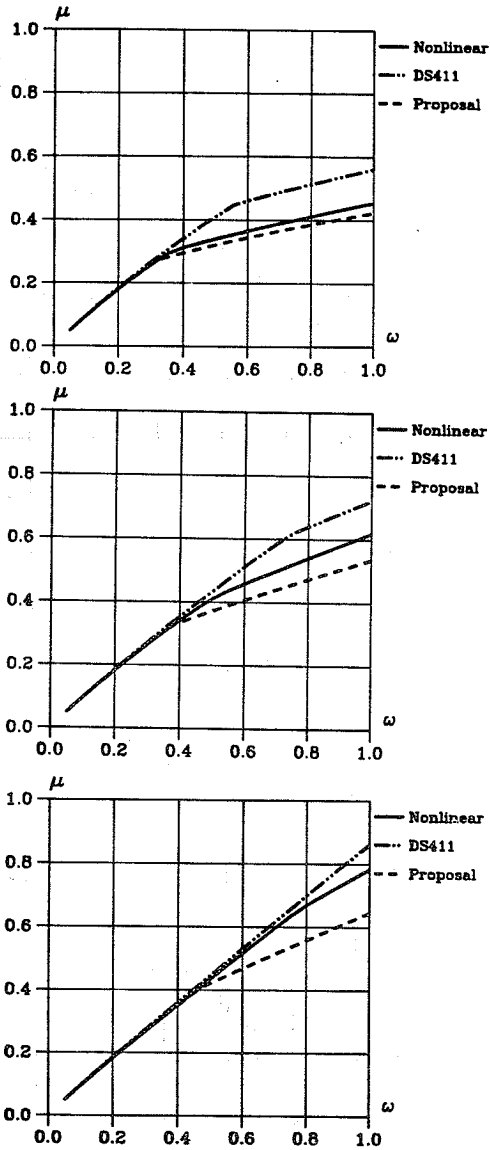


Fig. 5.13  $\mu$ - $\omega$  relationship of the Danish Code, DS 411, the proposal and the nonlinear model. The sections are subjected to pure bending and containing compressive steel ratios 0.2, 0.4 and 0.6 of the tensional steel amount. The concrete compressive strength of the section is on a 90 MPa level.

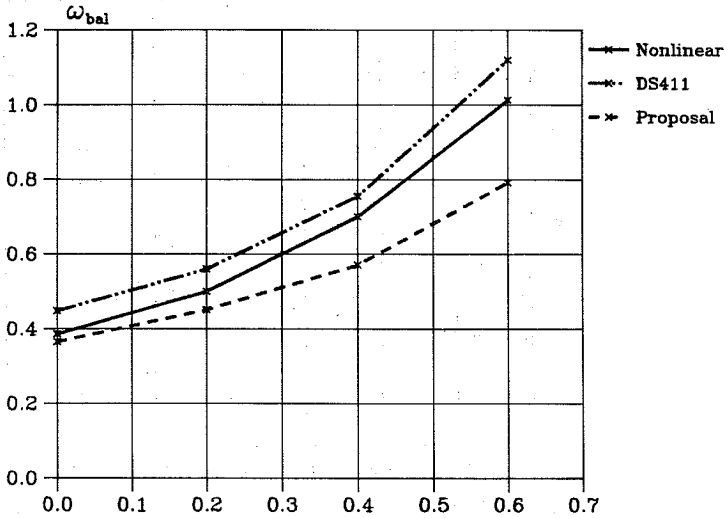


Fig. 5.14 Balanced mechanical tensional reinforcement ratio as a function of the compressive steel ratio in the case of sections subjected to pure bending and concrete compressive strength of the sections on a 40 MPa level.

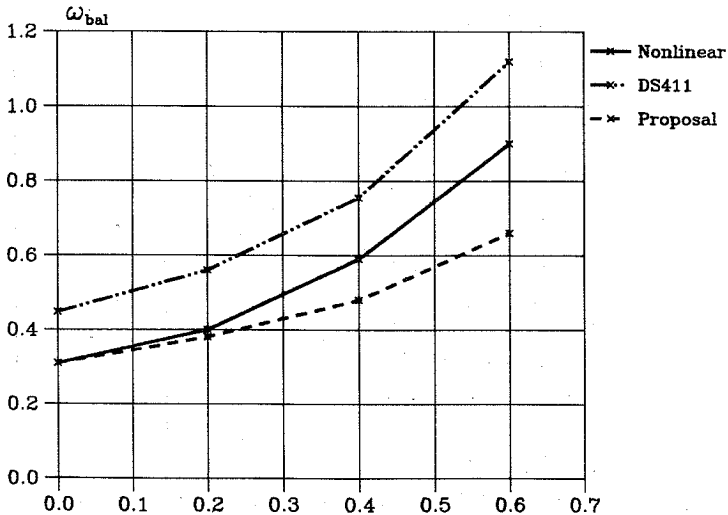


Fig. 5.15 Balanced mechanical tensional reinforcement ratio as a function of the compressive steel ratio in the case of sections subjected to pure bending and concrete compressive strength of the sections on a 50 MPa level.



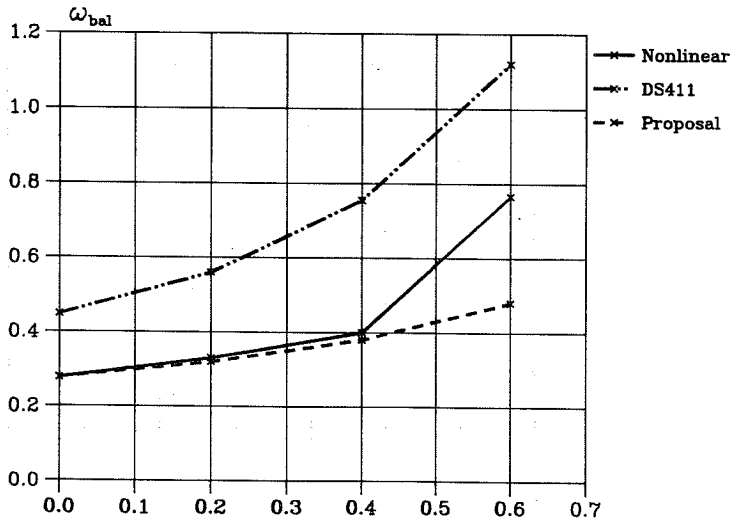


Fig. 5.16 Balanced mechanical tensional reinforcement ratio as a function of the compressive steel ratio in the case of sections subjected to pure bending and concrete compressive strength of the sections on a 60 MPa level.

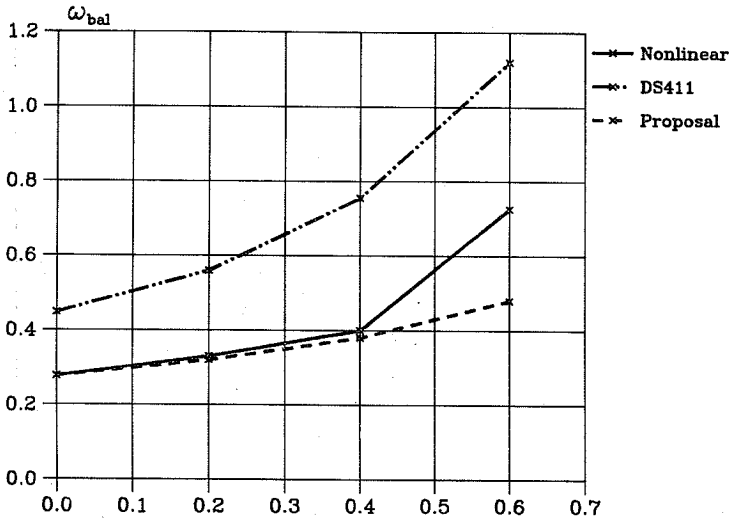


Fig. 5.17 Balanced mechanical tensional reinforcement ratio as a function of the compressive steel ratio in the case of sections subjected to pure bending and concrete compressive strength of the sections on a 70 MPa level.

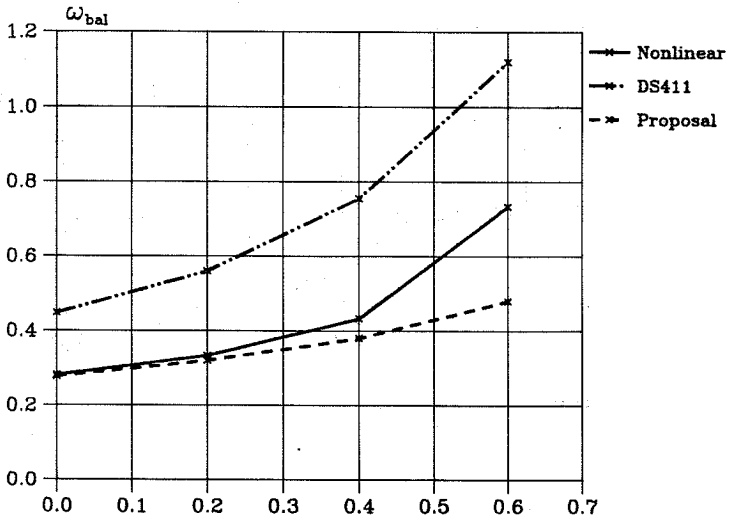


Fig. 5.18 Balanced mechanical tensional reinforcement ratio as a function of the compressive steel ratio in the case of sections subjected to pure bending and concrete compressive strength of the sections on a 80 MPa level.

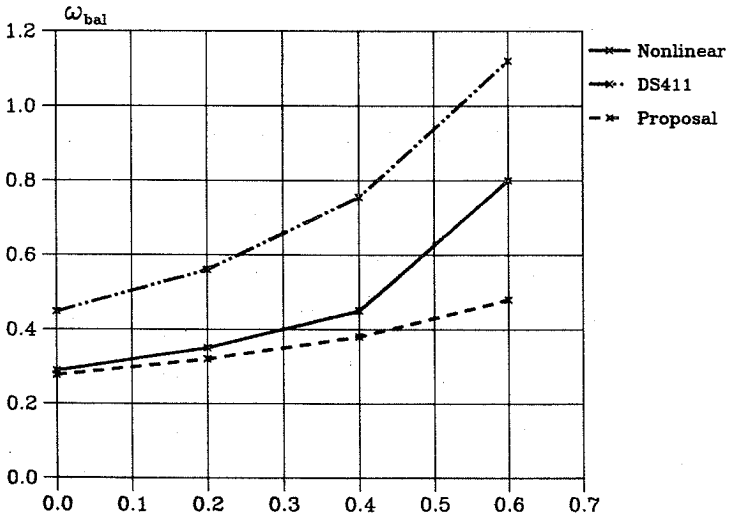


Fig. 5.19 Balanced mechanical tensional reinforcement ratio as a function of the compressive steel ratio in the case of sections subjected to pure bending and concrete compressive strength of the sections on a 90 MPa level.

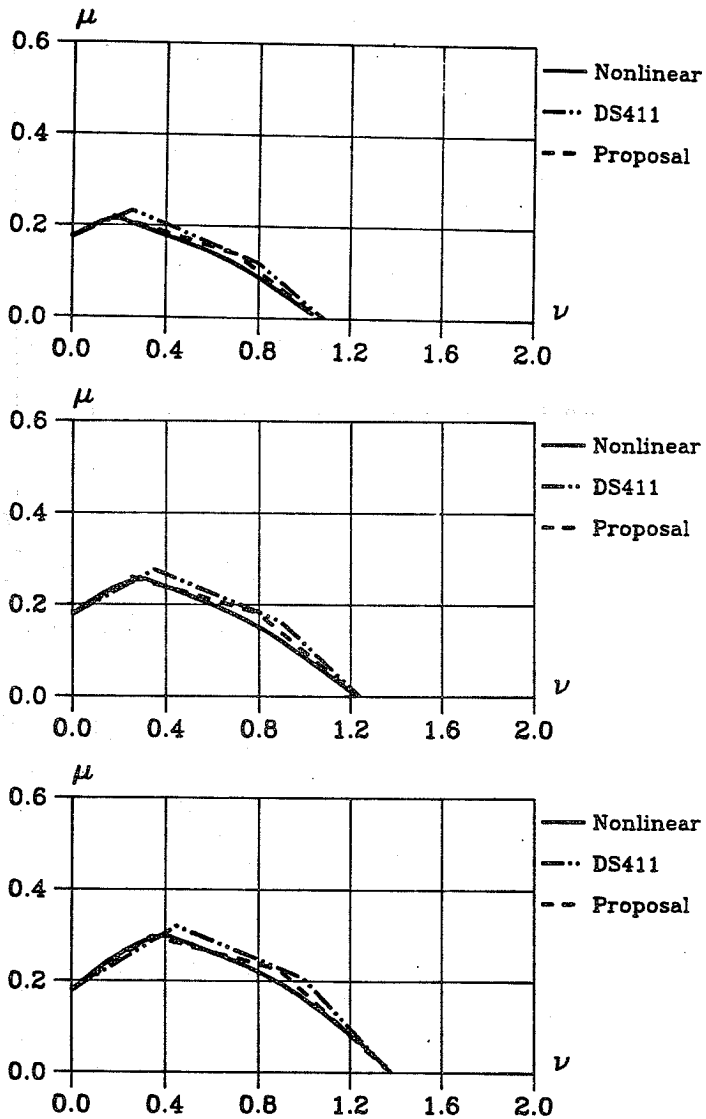


Fig. 5.20  $\mu$ - $\nu$  relationships of the Danish Code, DS 411, the proposal and the nonlinear model. The concrete compressive strength of the section is on a 40 MPa level. The section has a mechanical tensional steel ratio  $\omega = 0.5 \times \omega_{bal}$  and mechanical compressive steel ratio  $\omega_c = 0$ ,  $\omega_c = 0.5 \times \omega$  and  $\omega_c = \omega$ .

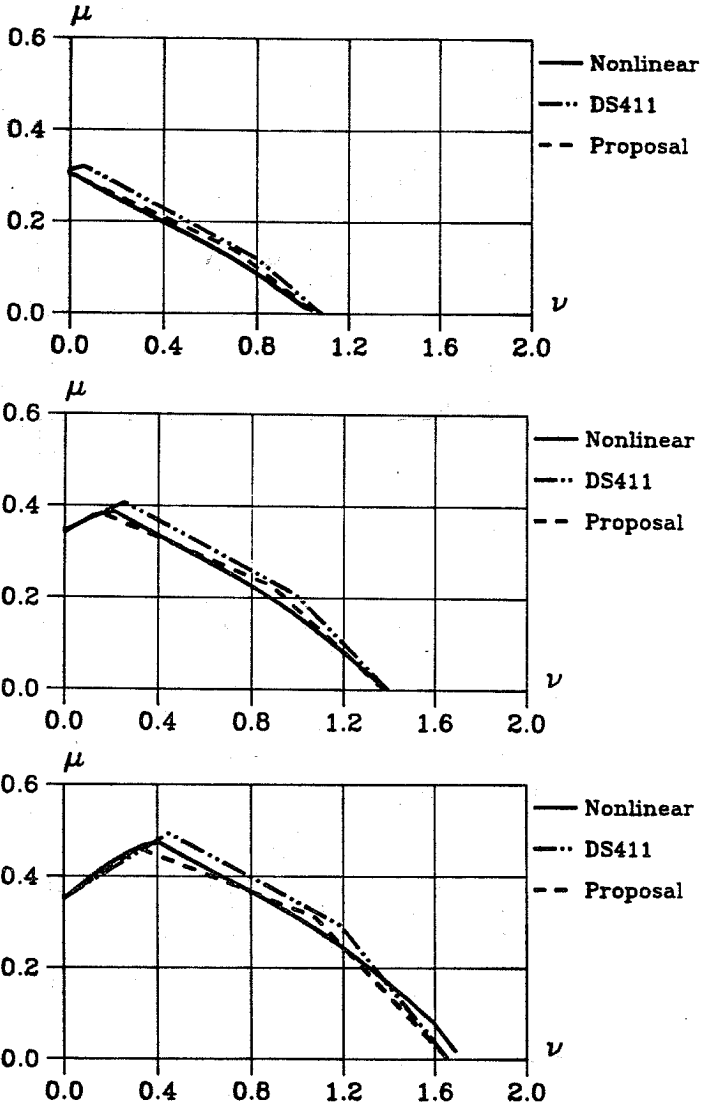


Fig. 5.21  $\mu$ - $\nu$  relationships of the Danish Code, DS 411, the proposal and the nonlinear model. The concrete compressive strength of the section is on a 40 MPa level. The section has a mechanical tensional steel ratio  $\omega = 1.0 \times \omega_{bal}$  and mechanical compressive steel ratio  $\omega_c = 0$ ,  $\omega_c = 0.5 \times \omega$  and  $\omega_c = \omega$ .

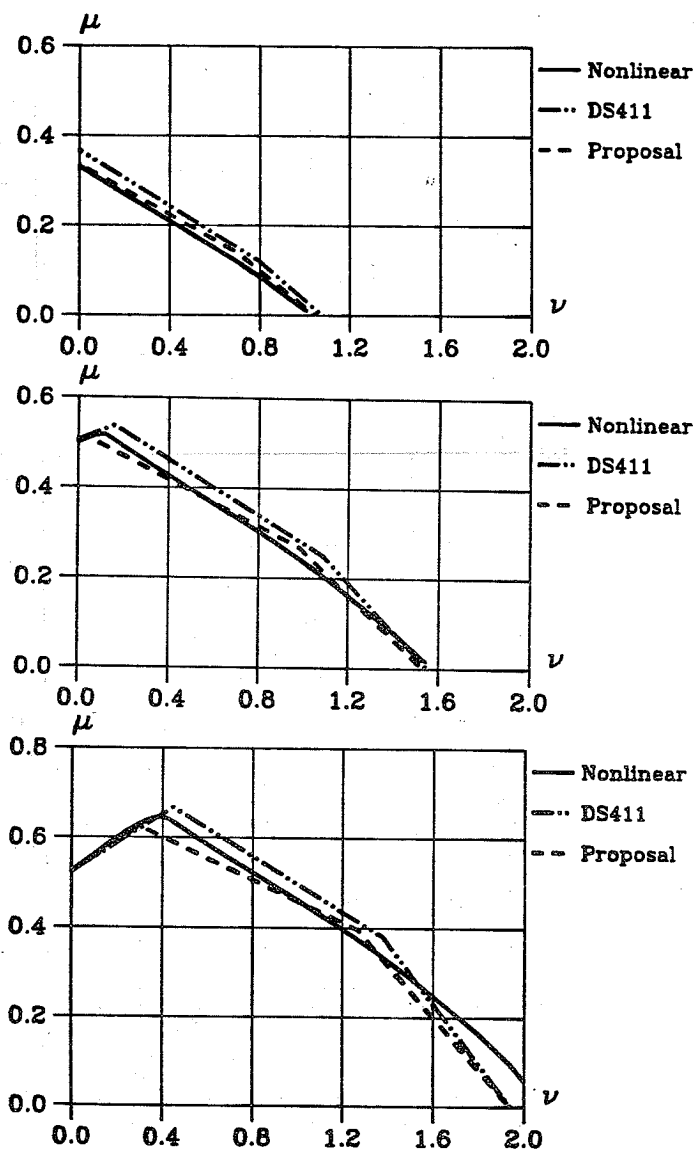


Fig. 5.22  $\mu$ - $\nu$  relationships of the Danish Code, DS 411, the proposal and the nonlinear model. The concrete compressive strength of the section is on a 40 MPa level. The section has a mechanical tensional steel ratio  $\omega = 1.5 \times \omega_{bal}$  and mechanical compressive steel ratio  $\omega_c = 0$ ,  $\omega_c = 0.5 \times \omega$  and  $\omega_c = \omega$ .

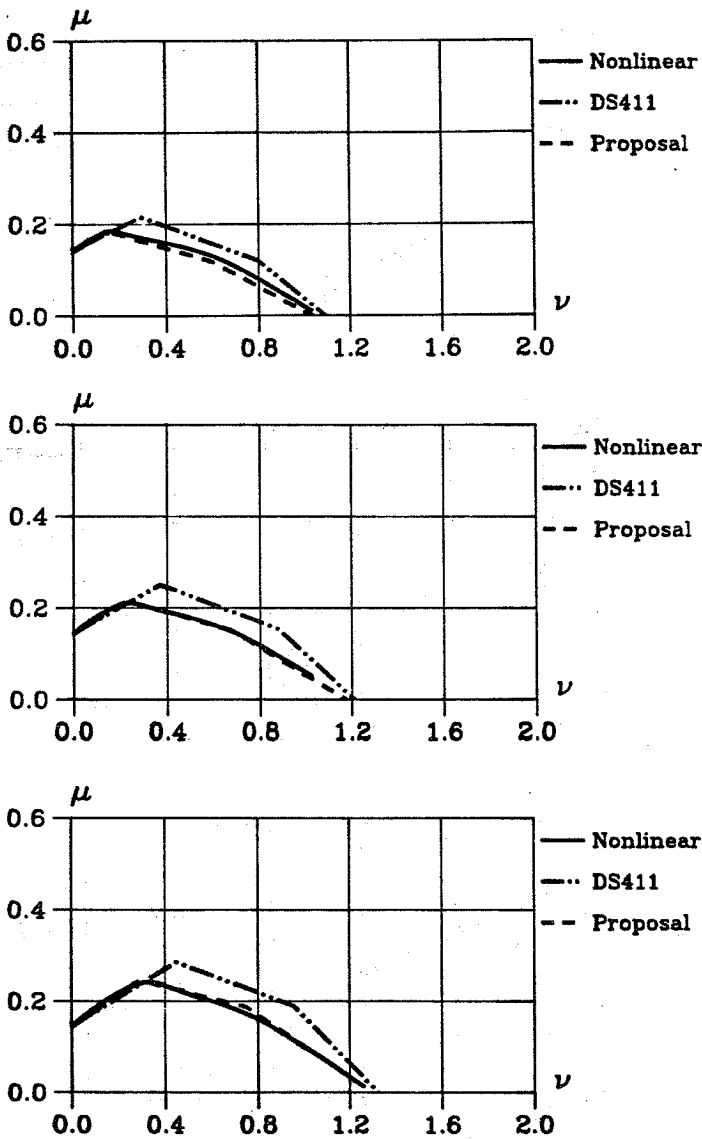


Fig. 5.23  $\mu$ - $\nu$  relationships of the Danish Code, DS 411, the proposal and the nonlinear model. The concrete compressive strength of the section is on a 50 MPa level. The section has a mechanical tensional steel ratio  $\omega = 0.5 \times \omega_{bal}$  and mechanical compressive steel ratio  $\omega_c = 0$ ,  $\omega_c = 0.5 \times \omega$  and  $\omega_c = \omega$ .

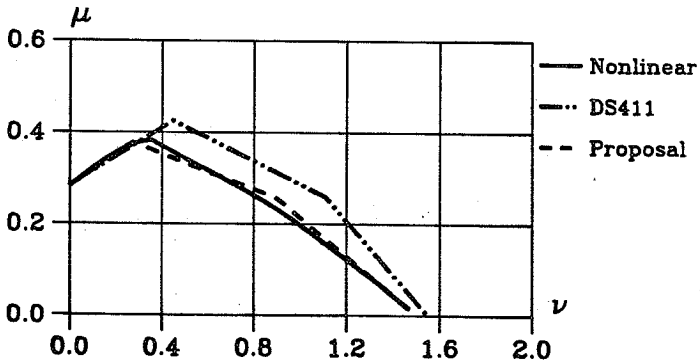
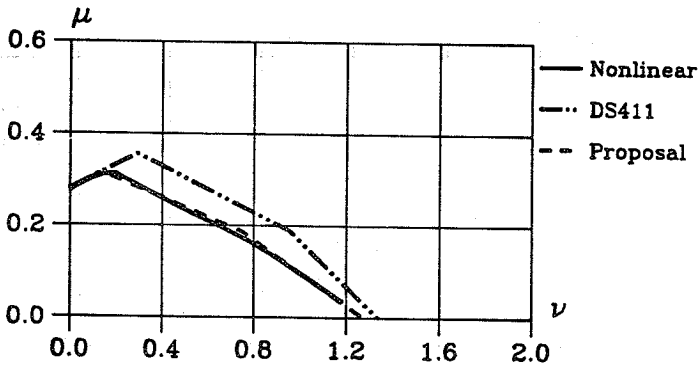
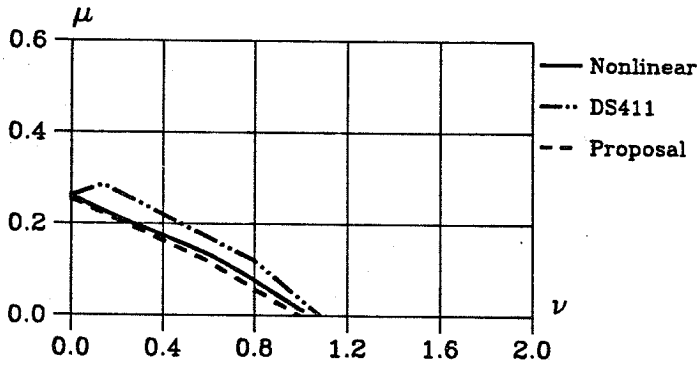


Fig. 5.24  $\mu$ - $\nu$  relationships of the Danish Code, DS 411, the proposal and the nonlinear model. The concrete compressive strength of the section is on a 50 MPa level. The section has a mechanical tensional steel ratio  $\omega = 1.0 \times \omega_{bal}$  and mechanical compressive steel ratio  $\omega_c = 0$ ,  $\omega_c = 0.5 \times \omega$  and  $\omega_c = \omega$ .

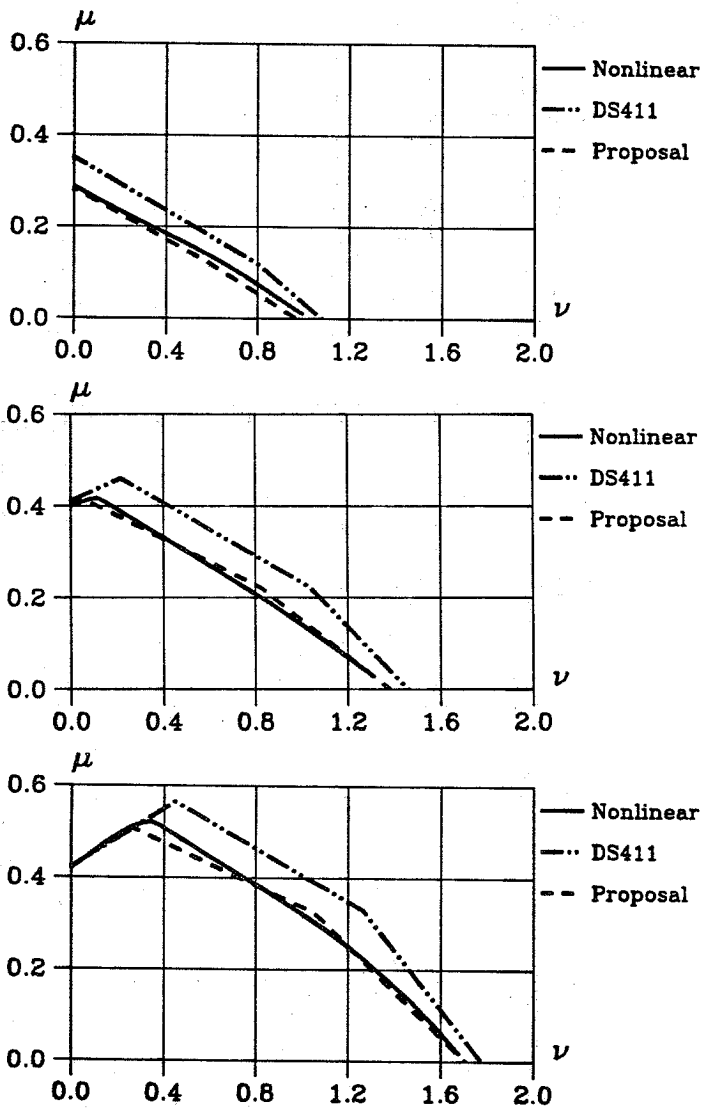


Fig. 5.25  $\mu$ - $\nu$  relationships of the Danish Code, DS 411, the proposal and the nonlinear model. The concrete compressive strength of the section is on a 50 MPa level. The section has a mechanical tensional steel ratio  $\omega = 1.5 \times \omega_{bal}$  and mechanical compressive steel ratio  $\omega_c = 0$ ,  $\omega_c = 0.5 \times \omega$  and  $\omega_c = \omega$ .



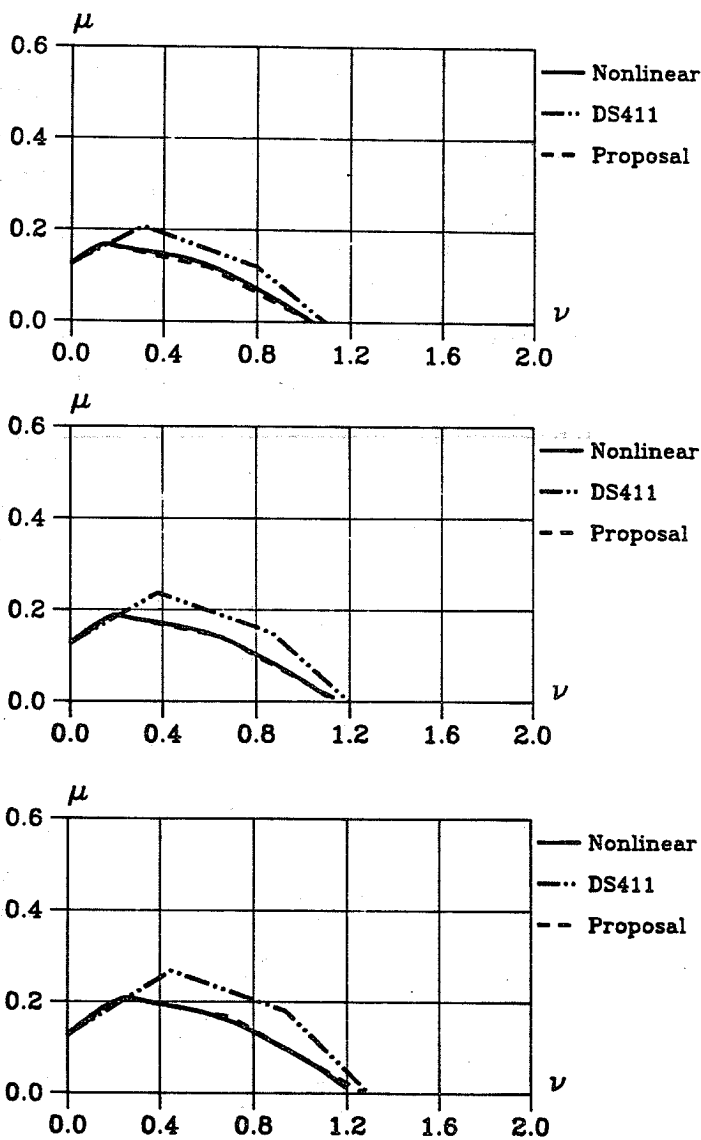


Fig. 5.26  $\mu$ - $\nu$  relationships of the Danish Code, DS 411, the proposal and the nonlinear model. The concrete compressive strength of the section is on a 60 MPa level. The section has a mechanical tensional steel ratio  $\omega = 0.5 \times \omega_{bal}$  and mechanical compressive steel ratio  $\omega_c = 0$ ,  $\omega_c = 0.5 \times \omega$  and  $\omega_c = \omega$ .

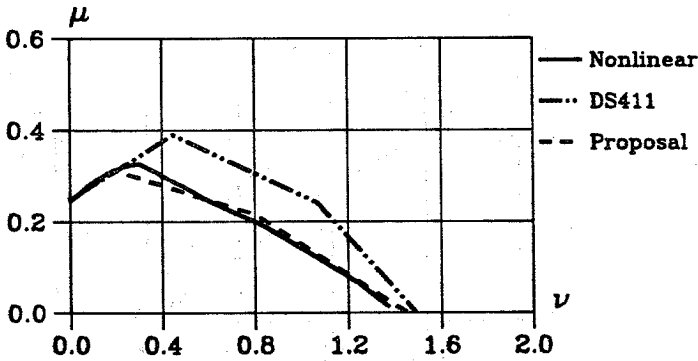
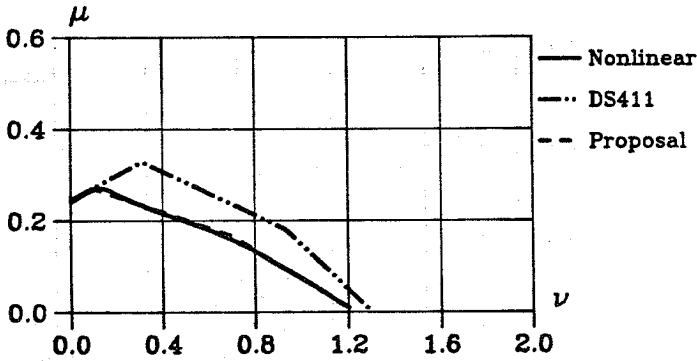
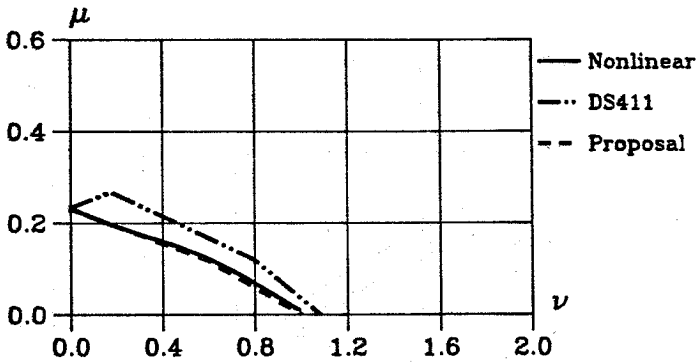


Fig. 5.27  $\mu$ - $\nu$  relationships of the Danish Code, DS 411, the proposal and the nonlinear model. The concrete compressive strength of the section is on a 60 MPa level. The section has a mechanical tensional steel ratio  $\omega = 1.0 \times \omega_{bal}$  and mechanical compressive steel ratio  $\omega_c = 0$ ,  $\omega_c = 0.5 \times \omega$  and  $\omega_c = \omega$ .

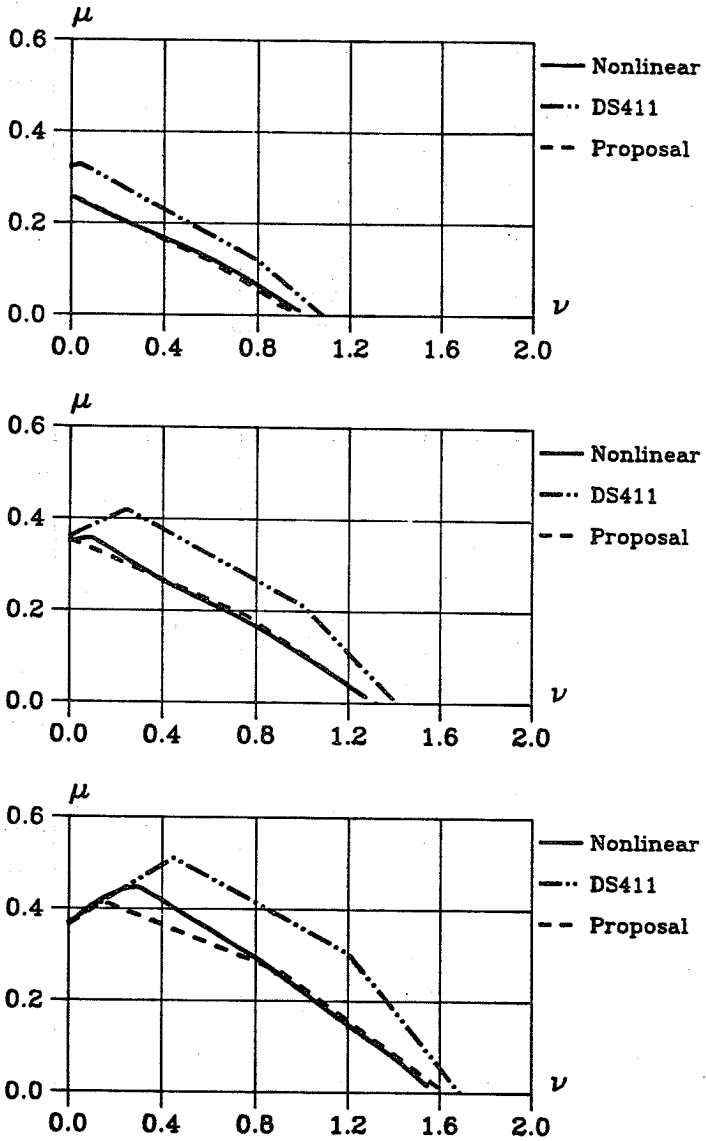


Fig. 5.28  $\mu$ - $\psi$  relationships of the Danish Code, DS 411, the proposal and the nonlinear model. The concrete compressive strength of the section is on a 60 MPa level. The section has a mechanical tensional steel ratio  $\omega = 1.5 \times \omega_{bal}$  and mechanical compressive steel ratio  $\omega_c = 0$ ,  $\omega_c = 0.5 \times \omega$  and  $\omega_c = \omega$ .

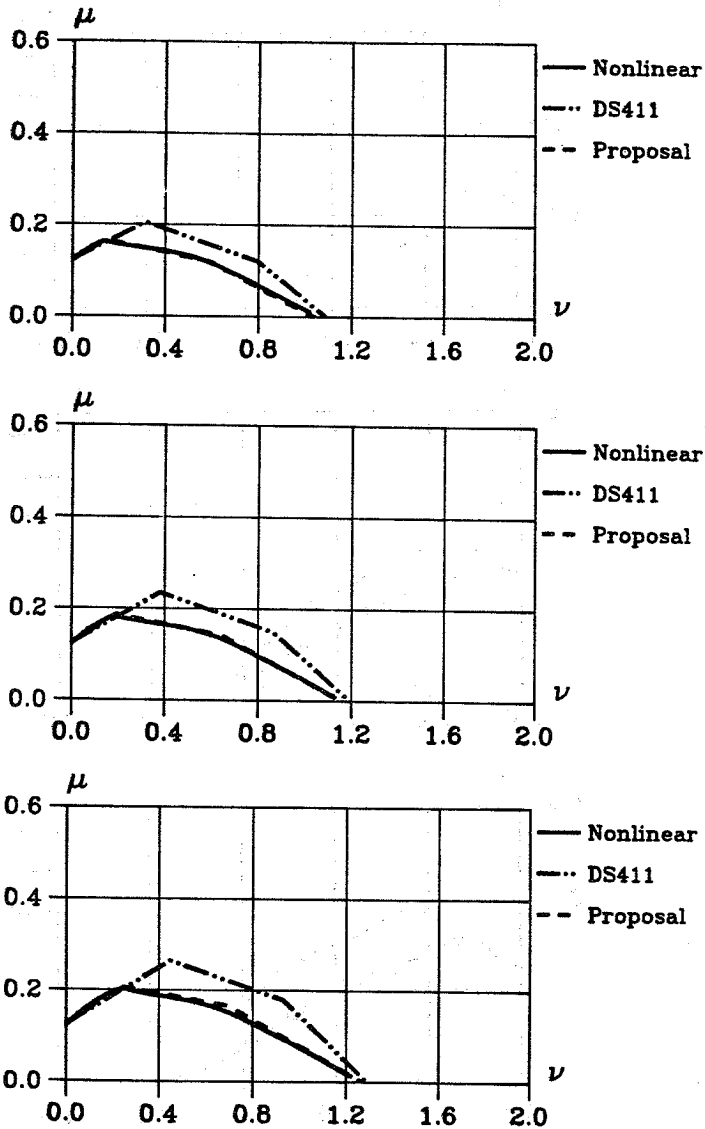


Fig. 5.29  $\mu$ - $\nu$  relationships of the Danish Code, DS 411, the proposal and the nonlinear model. The concrete compressive strength of the section is on a 70 MPa level. The section has a mechanical tensional steel ratio  $\omega = 0.5 \times \omega_{bal}$  and mechanical compressive steel ratio  $\omega_c = 0$ ,  $\omega_c = 0.5 \times \omega$  and  $\omega_c = \omega$ .

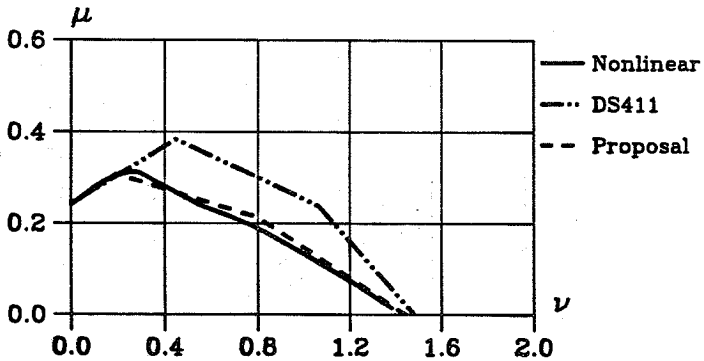
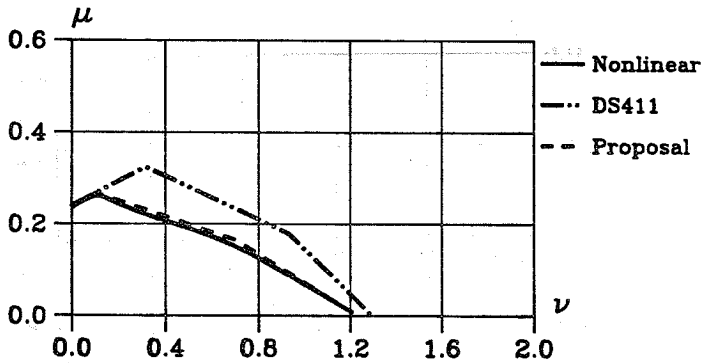
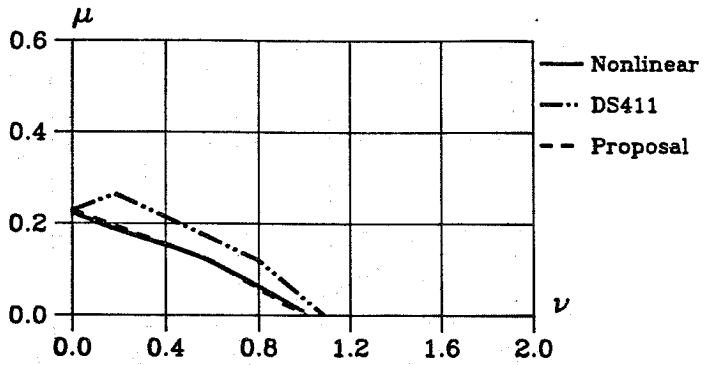


Fig. 5.30  $\mu$ - $\nu$  relationships of the Danish Code, DS 411, the proposal and the nonlinear model. The concrete compressive strength of the section is on a 70 MPa level. The section has a mechanical tensional steel ratio  $\omega = 1.0 \times \omega_{bal}$  and mechanical compressive steel ratio  $\omega_c = 0$ ,  $\omega_c = 0.5 \times \omega$  and  $\omega_c = \omega$ .

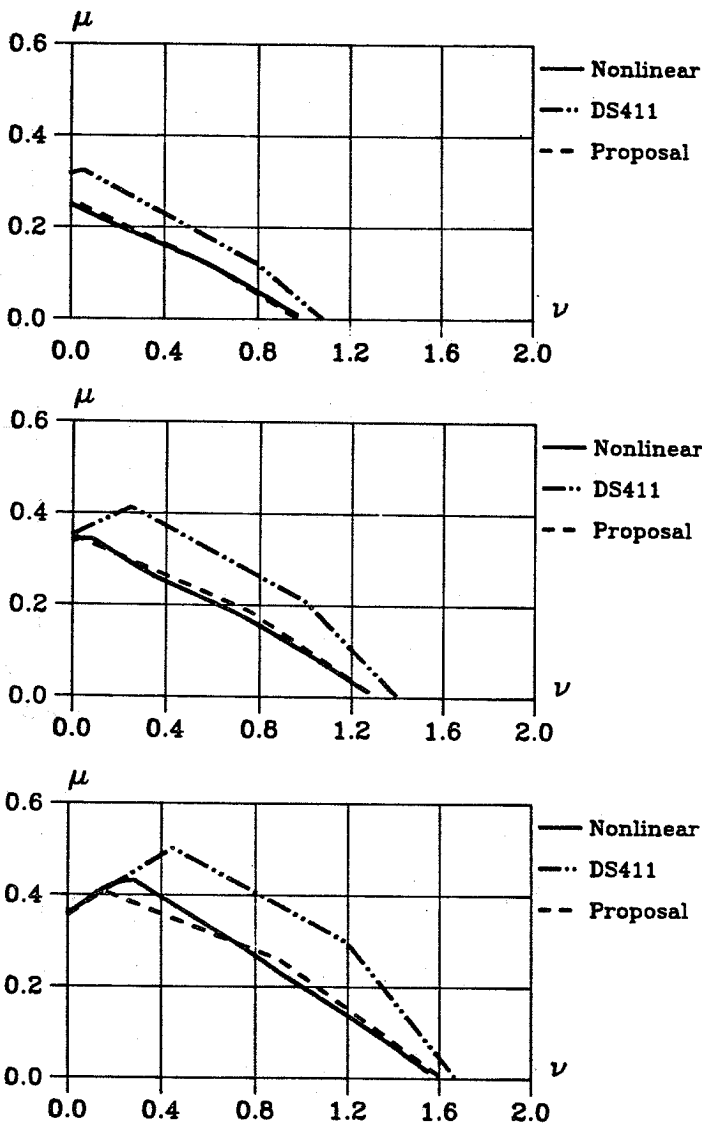


Fig. 5.31  $\mu$ - $\psi$  relationships of the Danish Code, DS 411, the proposal and the nonlinear model. The concrete compressive strength of the section is on a 70 MPa level. The section has a mechanical tensional steel ratio  $\omega = 1.5 \times \omega_{bal}$  and mechanical compressive steel ratio  $\omega_c = 0$ ,  $\omega_c = 0.5 \times \omega$  and  $\omega_c = \omega$ .

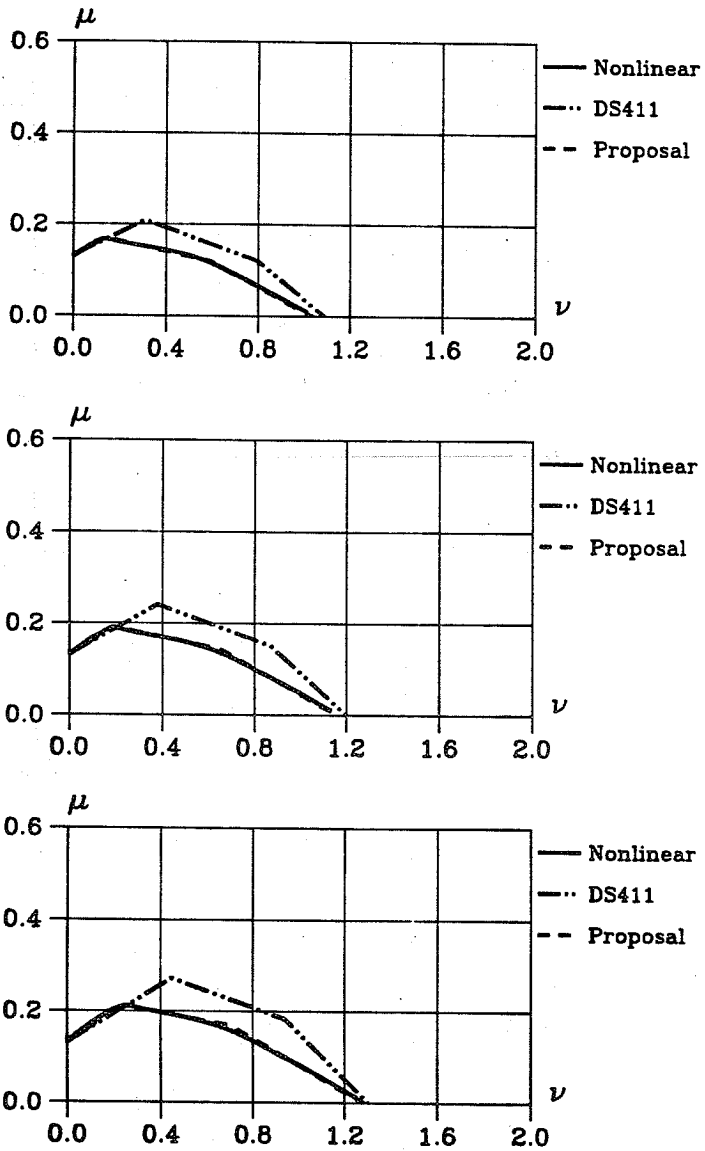


Fig. 5.32  $\mu$ - $\nu$  relationships of the Danish Code, DS 411, the proposal and the nonlinear model. The concrete compressive strength of the section is on a 80 MPa level. The section has a mechanical tensional steel ratio  $\omega = 0.5 \times \omega_{bal}$  and mechanical compressive steel ratio  $\omega_c = 0$ ,  $\omega_c = 0.5 \times \omega$  and  $\omega_c = \omega$ .

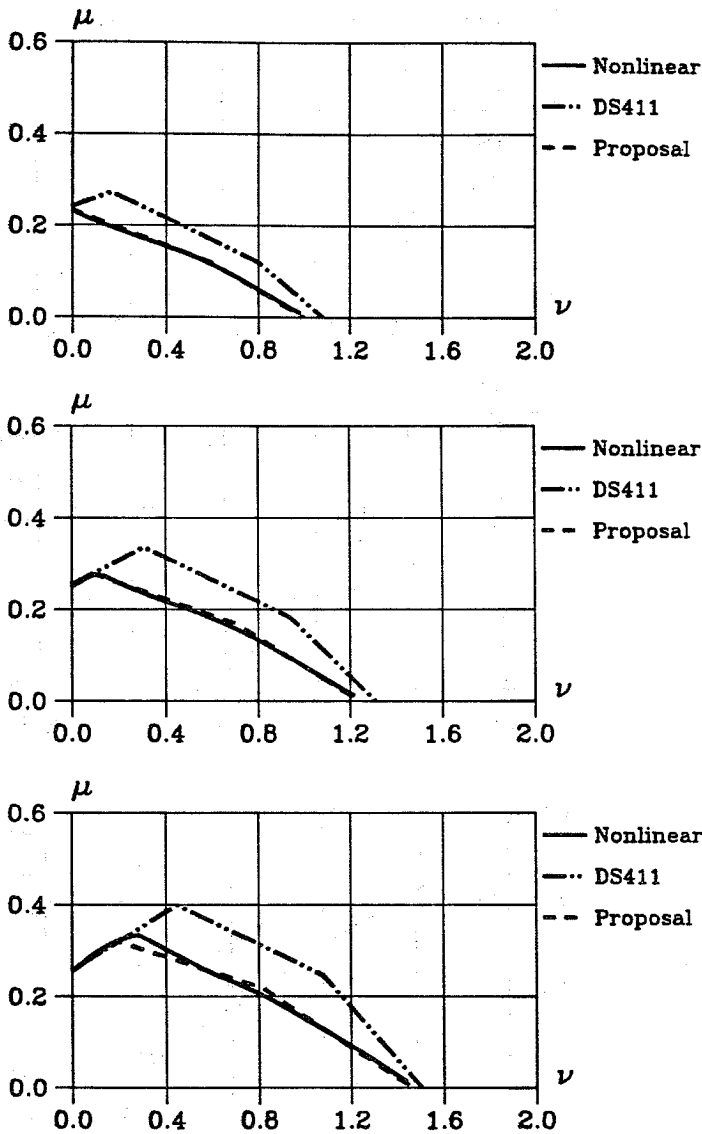


Fig. 5.33  $\mu$ - $\nu$  relationships of the Danish Code, DS 411, the proposal and the nonlinear model. The concrete compressive strength of the section is on a 80 MPa level. The section has a mechanical tensional steel ratio  $\omega = 1.0 \times \omega_{bal}$  and mechanical compressive steel ratio  $\omega_c = 0$ ,  $\omega_c = 0.5 \times \omega$  and  $\omega_c = \omega$ .



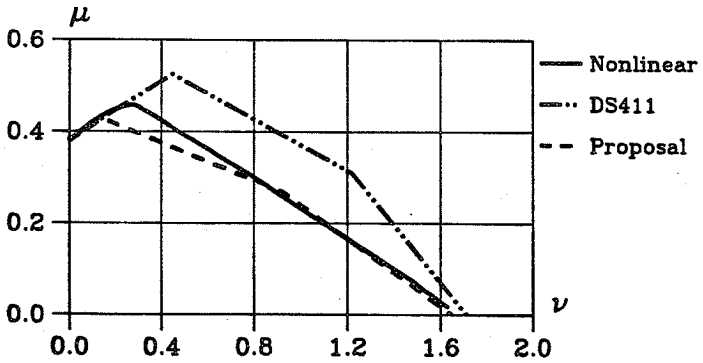
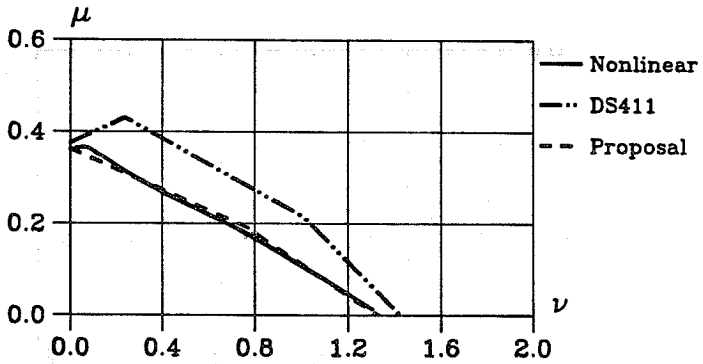
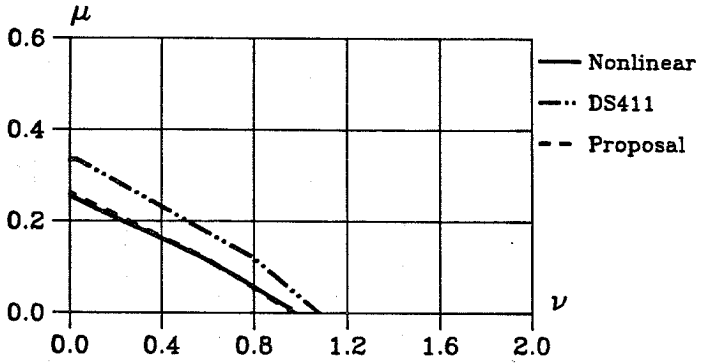


Fig. 5.34  $\mu$ - $\nu$  relationships of the Danish Code, DS 411, the proposal and the nonlinear model. The concrete compressive strength of the section is on a 80 MPa level. The section has a mechanical tensional steel ratio  $\omega = 0.5 \times \omega_{bal}$  and mechanical compressive steel ratio  $\omega_c = 0$ ,  $\omega_c = 0.5 \times \omega$  and  $\omega_c = \omega$ .

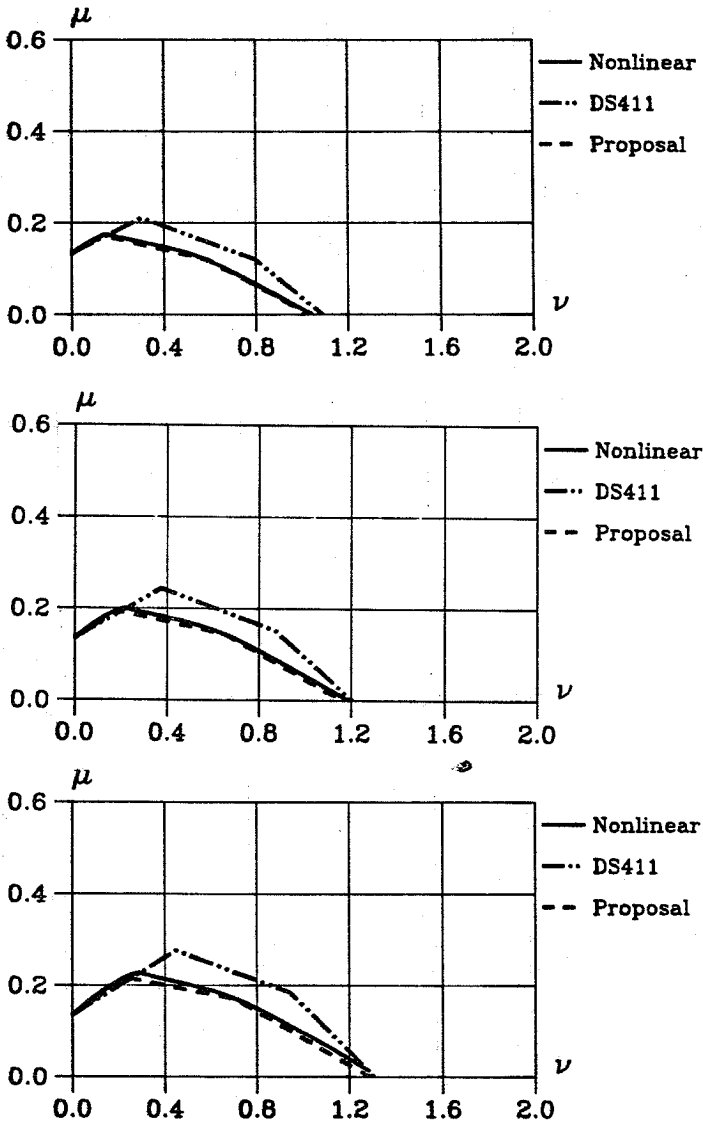


Fig. 5.35  $\mu$ - $\nu$  relationships of the Danish Code, DS 411, the proposal and the nonlinear model. The concrete compressive strength of the section is on a 90 MPa level. The section has a mechanical tensional steel ratio  $\omega = 0.5 \times \omega_{bal}$  and mechanical compressive steel ratio  $\omega_c = 0$ ,  $\omega_c = 0.5 \times \omega$  and  $\omega_c = \omega$ .

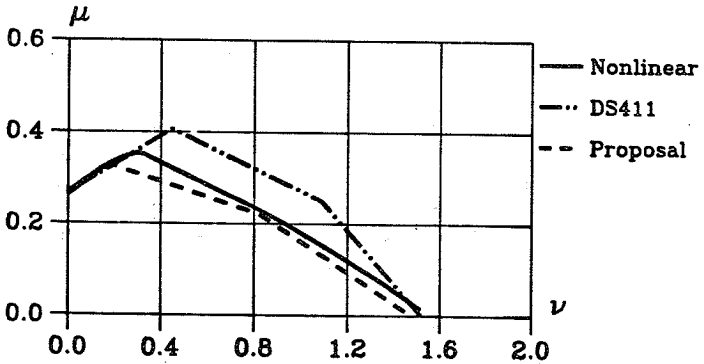
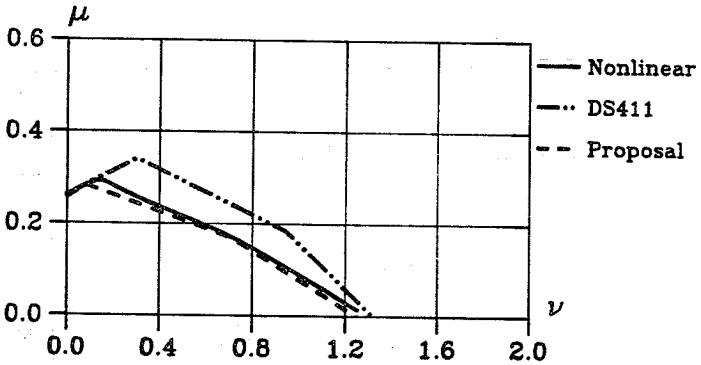
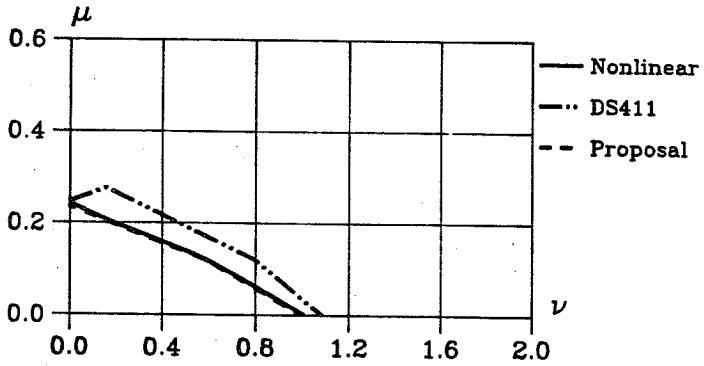


Fig. 5.36  $\mu$ - $\nu$  relationships of the Danish Code, DS 411, the proposal and the nonlinear model. The concrete compressive strength of the section is on a 90 MPa level. The section has a mechanical tensional steel ratio  $\omega = 1.0 \times \omega_{bal}$  and mechanical compressive steel ratio  $\omega_c = 0$ ,  $\omega_c = 0.5 \times \omega$  and  $\omega_c = \omega$ .

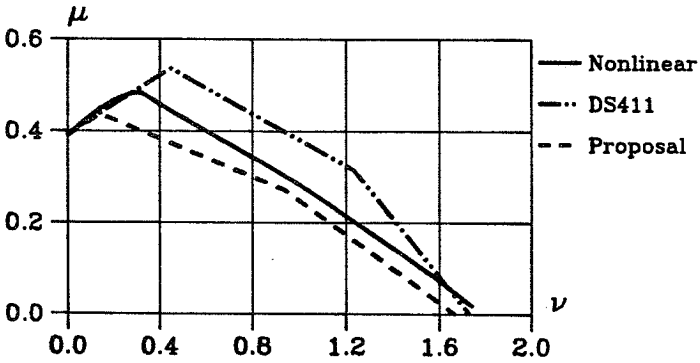
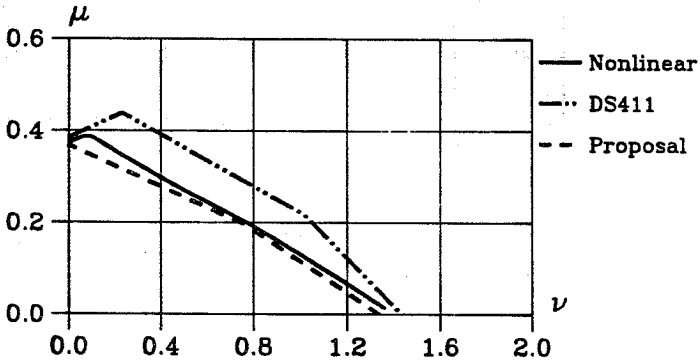
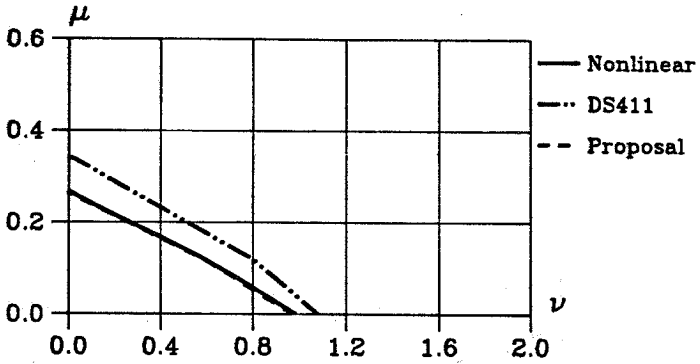


Fig. 5.37  $\mu$ - $\nu$  relationships of the Danish Code, DS 411, the proposal and the nonlinear model. The concrete compressive strength of the section is on a 90 MPa level. The section has a mechanical tensional steel ratio  $\omega = 1.5 \times \omega_{bal}$  and mechanical compressive steel ratio  $\omega_c = 0$ ,  $\omega_c = 0.5 \times \omega$  and  $\omega_c = \omega$ .

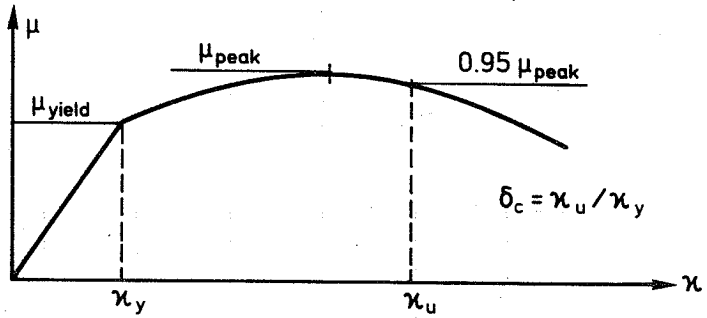


Fig. 6.1 Definition of ultimate curvature,  $\kappa_u$ , and curvature ductility index,  $\delta_c$ .

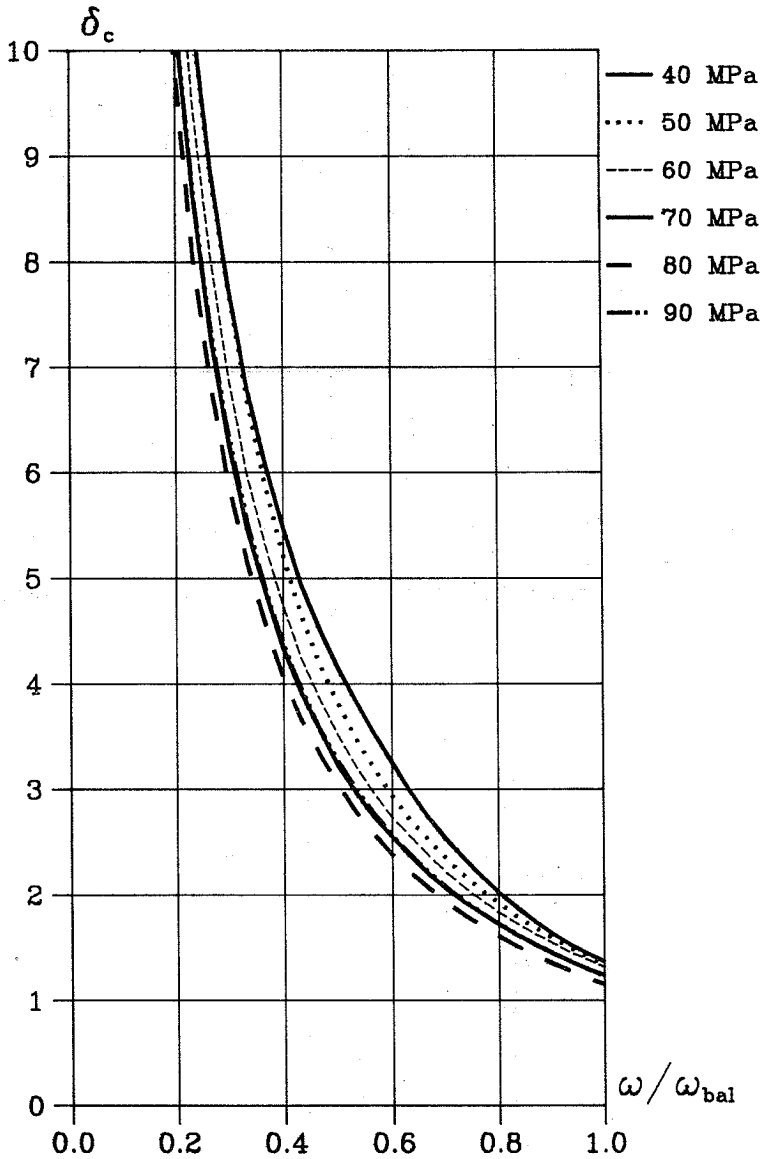


Fig. 6.2 Curvature ductility index,  $\delta_c$ , as a function of  $\omega/\omega_{bal}$ .

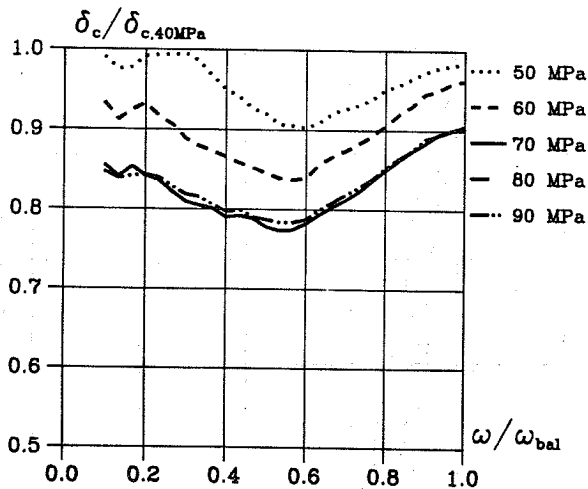


Fig. 6.3 Relative curvature ductility index,  $\delta_c / \delta_{c,40 MPa}$ , as function of  $\omega / \omega_{bal}$ , where  $\delta_{c,40 MPa}$  is the curvature ductility in the case of sections with concrete having compressive strength in a 40 MPa level.

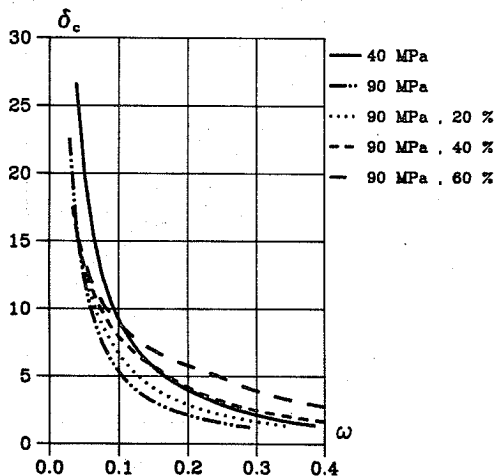


Fig. 6.4 Improvement of curvature ductility index by adding reinforcement in the compression zone of 90 MPa high strength concrete sections.

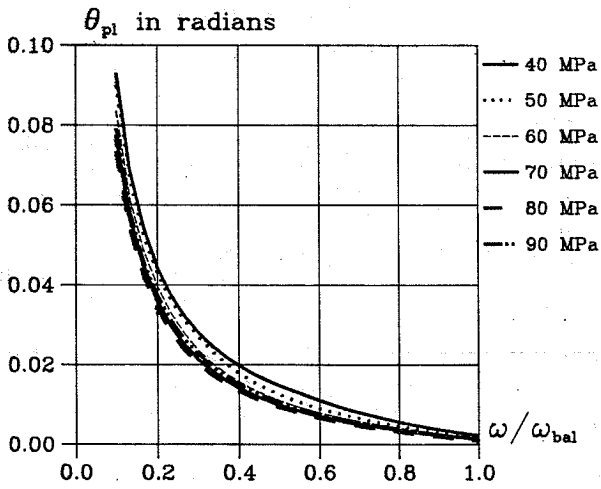


Fig. 6.5 Ultimate plasticity rotation,  $\theta_{pl}$  in radians, as a function of  $\omega/\omega_{bal}$ .



AFDELINGEN FOR BÆRENDE KONSTRUKTIONER  
DANMARKS TEKNISKE HØJSKOLE

Department of Structural Engineering  
Technical University of Denmark, DK-2800 Lyngby

SERIE R

(Tidligere: Rapporter)

- R 230. RIBERHOLT, H.: Woodflanges under tension, 1988.  
R 231. HOLKMANN OLSEN, N.: Implementation. 1988. (public pending).  
R 232. HOLKMANN OLSEN, N.: Uniaxial. 1988. (public pending)  
R 233. HOLKMANN OLSEN, N.: Anchorage. 1988. (public pending)  
R 234. HOLKMANN OLSEN, N.: Heat Induced. 1988. (public pending)  
R 235. SCHEEL, HELLE: Rotationskapacitet. 1988. (public pending)  
R 236. NIELSEN, MONA: Arbejdslinier. 1988. (public pending)  
R 237. GANWEI, CHEN: Plastic Analysis of Shear in Beams. Deep Beams and Corbels. 1988.  
R 238. ANDREASEN, BENT STEEN: Anchorage of Deformed Reinforcing bars. 1988.  
R 239. ANDREASEN, BENT STEEN: Anchorage Tests with deformed Reinforcing Bars in more than one layer at a Beam Support. 1988.  
R 240. GIMSING, N.J.: Cable-Stayed Bridges with Ultra Long Spans. 1988.  
R 241. NIELSEN, LEIF OTTO: En Reissner-Mindlin Plade Element Familie. 1989.  
R 242. KRENK, STEEN og THORUP, ERIK: Stochastic and Concrete Amplitude Fatigue Test of Plate Specimens with a Central Hole. 1989.  
R 243. AARKROG, P., THORUP, E., KRENK, S., AGERSKOV, H. and BJØRN-BAK-HANSEN, J.: Apparatur til Udmattelsesforsøg. 1989.  
R 244. DITLEVSEN, OVE and KRENK, STEEN: Research Workshop on Stochastic Mechanics, September 13-14, 1988.  
R 245. ROBERTS, J.B.: Averaging Methods in Random Vibration. 1989.  
R 246. Resumeoversigt 1988 - Summaries of Papers 1988. 1989.  
R 247. GIMSING, N.J., JAMES D. LOCKWOOD, JAEHO SONG: Analysis of Erection Procedures for Cable-Stayed Bridges. 1989.  
R 248. DITLEVSEN, O. og MADSEN, H.O.: Proposal for a Code for the Direct Use of Reliability Methods in Structural Design. 1989.  
R 249. NIELSEN, LEIF OTTO: Simplex Elementet. 1989.  
R 250. THOMSEN, BENTE DAHL: Undersøgelse af "shear lag" i det elasto-plastiske stadium. 1990.  
R 251. FEDDERSEN, BENT: Jernbetonbjælkens bæreevne. 1990.  
R 252. FEDDERSEN, BENT: Jernbetonbjælkens bæreevne, Appendix. 1990.  
R 253. AARKROG, PETER: A Computer Program for Servo Controlled Fatigue Testing Documentation and User Guide. 1990.  
R 254. HOLKMANN OLSEN, DAVID & NIELSEN, M.P.: Ny Teori til Bestemmelse af Revneafstande og Revnevidder i Betonkonstruktioner. 1990.  
R 255. YAMADA, KENTARO & AGERSKOV, HENNING: Fatigue Life Prediction of Welded Joints Using Fracture Mechanics. 1990.  
R 256. Resumeoversigt 1989 - Summaries of Papers 1989. 1990.  
R 257. HOLKMANN OLSEN, DAVID, GANWEI, CHEN, NIELSEN, M.P.: Plastic Shear Solutions of Prestressed Hollow Core Concrete Slabs. 1990.  
R 258. GANWEI, CHEN & NIELSEN, M.P.: Shear Strength of Beams of High Strength Concrete. 1990.  
R 259. GANWEI, CHEN, NIELSEN, M.P. NIELSEN, JANOS, K.: Ultimate Load Carrying Capacity of Unbonded Prestressed Reinforced Concrete Beams. 1990.  
R 260. GANWEI, CHEN, NIELSEN, M.P.: A Short Note on Plastic Shear Solutions of Reinforced Concrete Columns. 1990.  
R 261. GLUVER, HENRIK: One Step Markov Model for Extremes of Gaussian Processes. 1990.

Abonnement 1.7.1990 - 30.6.1991 kr. 130,-  
Subscription rate 1.7.1990 - 30.6.1991 D.Kr. 130.-.